

Lisa Theisl, BSc

**Generating a new EAE model involving cortical lesions with close  
resemblance to human multiple sclerosis**

**MASTER'S THESIS**

to achieve the university degree of

Master of Science

Master's degree programme: Biochemistry and Molecular Biomedical Sciences

submitted to

**Graz University of Technology**

Supervisor

Ass.-Prof. Priv.-Doz. Dr.med.univ. Dr.rer.nat. Sonja Hochmeister

Medical University Graz

## AFFIDAVIT

I declare that I have authored this thesis independently, that I have not used other than the declared sources/resources, and that I have explicitly indicated all material which has been quoted either literally or by content from the sources used. The text document uploaded to TUGRAZonline is identical to the present master's thesis dissertation.

29.02.2016

Date

Heisl Lisa

Signature

## **Acknowledgement**

First and foremost I offer my sincerest gratitude to my supervisor, Dr Sonja Hochmeister, who has supported me throughout my thesis with her patience and knowledge. I attribute the level of my Master's degree to her encouragement and effort and without her, this thesis, too, would not have been completed or written.

I would also like to thank the experts who were performing the MRI scans for this research project: Dr Stefan Ropele and Johannes Strasser. Without their passionate participation and input, the MRI scans could not have been successfully conducted.

Special thanks go to Michaela Haindl. Without her influence I would not have written this thesis. To be honest I simply could not, she was the one who shared her knowledge with me. She showed me how to work with Leica, my little friend. She also never hesitated to help me with any sort of problems I had throughout the practical part of my thesis.

I would also like to thank Alex Schossmann, who often had to bear my burst of frustration and rages against the world and Microsoft Office. As a physicist he always tried to understand what is going on in the world of a biochemist.

Finally, I must express my very profound gratitude to my parents, Irene and Gottfried Theisl, for providing me with unfailing support and continuous encouragement throughout my years of study and through the process of researching and writing this thesis. This accomplishment would not have been possible without them. Thank you.

Lisa Theisl

## Kurzfassung

Multiple Sklerose (MS) ist eine häufige demyelinisierende Erkrankung, die das zentrale Nervensystem (ZNS) von überwiegend jungen Erwachsenen betrifft. Als Ursache wird ein autoimmuner Prozess in Betracht gezogen, jedoch sind die exakten Krankheitsmechanismen noch nicht vollständig aufgeklärt. MS zeichnet sich pathologisch- histologisch durch Entzündung, Demyelinisierung, axonalem Verlust und Gliose aus; diese Herde könne prinzipiell überall im zentralen Nervensystem der Betroffenen auftreten. Prädilektionsstellen sind allerdings die Sehnerven, die weiße Substanz periventrikulär sowie im Rückenmark. Daneben kommen, vorallem in späteren Krankheitsstadien, auch Läsionen im Kortex hinzu, die viel zu den klinischen Gesamteinschränkungen beitragen und sich histopathologisch von den Läsionen in der weißen Substanz unterscheiden.

Zur Pathogenese von kortikalen Läsionen in der MS ist wenig bekannt. Ein Grund dafür ist, dass sich die verfügbaren Tiermodelle der MS nicht oder nicht regelmäßig auf den Kortex auswirken. In dieser Masterarbeit versuchte man ein neues Tiermodell zu entwerfen, das regelmäßig Läsionen im Kortex, aber keine Läsionen der weißen Substanz verursacht.

Für diese Studie wählte man die Dark Agouti (DA) Ratte als Tiermodell aus. Zunächst implantierte man einen Katheter in die rechte zerebrale Hemisphäre, um Zugang zum Kortex zu erlangen. Nach einer Einheilungsphase wurden die DA Ratten subklinisch mit Myelin Oligodendrozyten Glykoprotein (MOG), einem Myelinbestandteil, immunisiert. Danach folgte die selektive Öffnung der Blut-Hirn-Schranke durch die Gabe einer inflammatorischen Zytokinmischung über den implantierten Katheter. Anschließend wurden serielle MRT-Aufnahmen sowie histologische und immunohistochemische Untersuchungen durchgeführt. Wir zeigen die selektive ausgedehnte Demyelinisierung im zerebralen Kortex unserer Versuchstiere ohne Rückenmarksbeteiligung. Die sonst üblichen aufsteigenden Lähmungserscheinungen in den Tieren, die oftmals die Versuchsdauer limitieren, entfallen.

## **Abstract**

Multiple sclerosis (MS) is the most common demyelinating disease affecting the central nervous system (CNS) of young adults. The cause for MS is considered to be an autoimmune process, though the exact mechanisms are still not completely understood. MS is characterized by inflammation, demyelination, axonal loss and gliosis. However demyelination, which causes the focal destruction of the myelin sheaths, is the hallmark of this disease. Recent studies suggested that cortical lesions contribute much to the overall disability of this disease, especially in late stages of the disease. The pathogenesis of the cortical lesion formation is largely unknown. One reason for this is that the available animal models of MS do not usually affect the cortex. In this master thesis we were trying to create a new rodent animal model that shows predictable and constant cortical lesions. So this model has a closer resemblance to the human MS, at least in this histopathological aspect. For this study we chose the Dark Agouti (DA) rats as our animal model. First we were implanting a catheter into the right cerebral hemisphere to have access to the cortex. After a certain healing phase the DA rats were actively immunised with Myelin Oligodendrocyte Glycoprotein (MOG). This was followed by the opening of the blood brain barrier (BBB) with the administration of an inflammatory cytokine mixture via the implanted catheter. Afterwards we performed serial MRI scans and histological and immunohistochemical examination. As a result we were able to create a new focal cortical animal model of MS that shows reproducible demyelination in the cortex but not in the spinal cord.

## Table of contents

1. Multiple Sclerosis .....	1
2. Myelin .....	2
2.1 Formation of the myelin sheath .....	3
2.2 Proteolipid protein (PLP) .....	5
2.3 Myelin basic protein (MBP) .....	5
2.3.1 PLP, MBP and multiple sclerosis.....	6
2.4 Myelin – associated glycoprotein (MAG) .....	6
2.5 2',3'-cyclic nucleotide 3'-phosphodiesterase (CNP-ase) .....	6
2.6 Myelin – oligodendrocyte glycoprotein (MOG).....	7
3. Experimental models of MS .....	7
3.1 Experimental allergic encephalomyelitis (EAE) .....	7
3.1.1 Animal strains and their characteristics .....	10
3.1.2 Differences between MS and EAE .....	13
3.2 Virus – induced inflammatory demyelinating diseases .....	14
3.2.1 Theiler's murine encephalomyelitis virus (TMEV).....	14
3.2.2 Mouse hepatitis virus (MHV) .....	15
3.3 Toxic models of MS .....	15
3.4 Limitations of animal models in MS.....	16
4. Aim of this thesis: Generating a new model involving cortical lesions with close resemblance to human MS .....	17
5. Material and methods .....	18
5.1 Animals.....	18
5.2 Catheter implantation.....	18
5.3 Immunization procedure.....	19
5.4 Enzyme-linked immunosorbent assay (ELISA) .....	19
5.5 Opening of the blood brain barrier (BBB) .....	20
5.6 Magnetic Resonance Imaging (MRI) .....	20
5.6.1 Animals anaesthesia during MRI scans.....	21
5.7 Histopathology .....	21
5.7.1 Fixation .....	21
5.7.2 Haematoxylin and eosin (HE).....	22

5.7.3	Luxol fast blue (LFB) .....	23
5.8	Immunohistochemistry (IHC).....	24
5.8.1	Epitope/Antigen retrieval .....	25
5.8.2	Blocking .....	25
5.8.3	Avidin-biotin complex (ABC) and labelled avidin-biotin method: .....	25
5.8.4	IHC staining protocol.....	26
6.	Results.....	28
6.1	The catheter itself does not cause any adverse tissue reaction.....	28
6.2	Clinical signs and symptoms of the animals .....	30
6.3	Serial MRI scans.....	30
6.4	Histopathology and immunohistochemistry shows a widespread demyelination of the cortex.....	33
6.5	Post mortem MRI scans.....	36
7.	Discussion.....	37
8.	List of figures.....	41
9.	List of references .....	44

## 1. Multiple Sclerosis

Multiple sclerosis (MS) is the most common demyelinating disease affecting the central nervous system (CNS) of young adults (Compston, et al., 1998). MS is characterized by inflammation, demyelination, axonal loss and gliosis. Generally autoimmune-mediated inflammation is believed to be the main trigger of events that lead to CNS tissue damage. Demyelination, the focal destruction of the myelin sheaths, is the hallmark of MS (Constantinescu, et al., 2011; Merkler, et al., 2006). Therefore the demyelinated plaque is the essential brain lesion in MS. The demyelinated plaque can occur anywhere in the CNS where myelin sheaths are present. The demyelination process goes along with astrocytosis and the formation of scars as reflected in the name of the disease. There are sclerotic plaques which are widely spread throughout the brain and spinal cord as well (Compston, et al., 1998). Nevertheless there is a certain amount of re-myelination, which offers hope for therapies. Further researches are aimed to enhance endogenous repair mechanisms (Constantinescu, et al., 2011) (Harlow, et al., 2015).

Clinically MS manifests itself as neurological deficits that exhibit a relapsing and remitting pattern. It can resolve completely or leave residual deficits. The deficits include any part of the CNS alone or in combination. The most common manifestations are somatosensory, pyramidal-motor and visual manifestations (Constantinescu, et al., 2011; Murray, 2005).

However there is a great diversity of the signs and symptoms for MS (Compston, et al., 1998). There are many MS subtypes existing: The relapsing-remitting MS (RRMS) type is the most common type and is characterized by multiple relapses of the disease followed by recovery. The phase of the disease where a gradual neurological progression follows a period of RRMS is known as secondary progressive MS (SPMS). Primary progressive MS (PPMS) affects ~15% of people suffering from MS. The steady neurological progression is in this case present from onset. In many cases superimposed relapses do not occur. Progressive-relapsing MS is a very rare subtype. The gradual PPMS-like course is covered with a few acute exacerbations (Constantinescu, et al., 2011; Joy, et al., 2001).



The cause for MS is considered to be an autoimmune process. T-lymphocytes with receptors for CNS myelin components enter the brain and undergo a local clonal expansion and attack local cells. The result is an inflammatory cascade which is responsible for the neurological deficits (Compston, et al., 1998; Murray, 2005).

.

## **2. Myelin**

Myelin (figure 1), the main target of the disease process in MS, consists of ~80% lipids and ~20% proteins (Rasband, 2015). Cholesterol, phospholipid and galactolipid are the major lipids. The two major myelin proteins are proteolipid protein (PLP) and myelin basic protein (MBP). Myelin-associated glycoprotein (MAG), myelin-oligodendrocyte glycoprotein (MOG) and 2',3'-cyclic nucleotide 3'-phosphodiesterase (CNP-ase) are forming the minor protein fraction (Compston, et al., 1998; Siegel, et al., 1999).

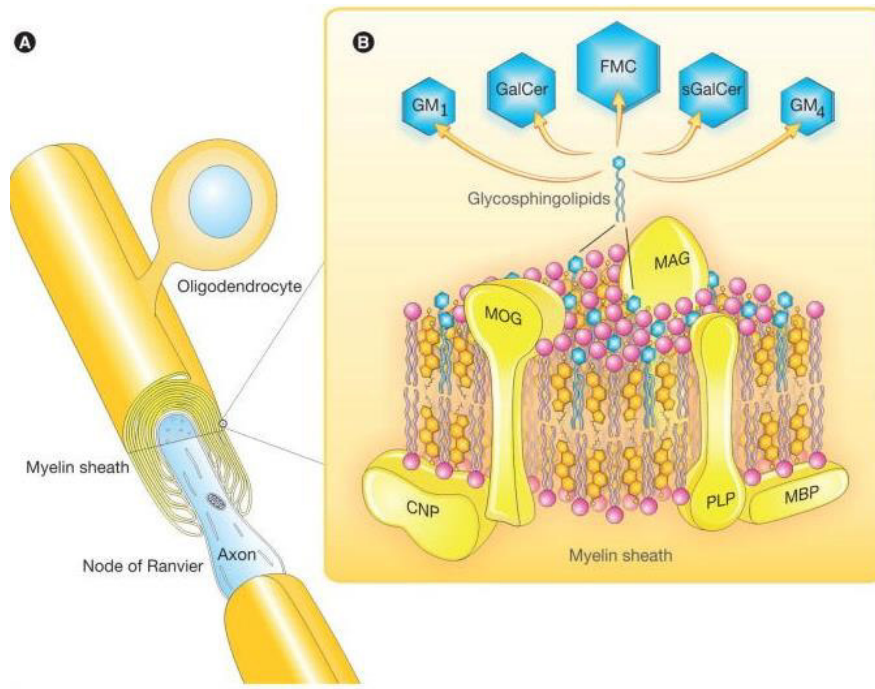


**Figure 1: CNS myelin and its components. (A)** An oligodendrocyte and myelin sheath in the CNS is shown. This version is simplified and has fewer myelin sheaths per oligodendrocyte. **(B)** 3D molecular composition of CNS myelin. Myelin proteins (MAG, MOG, PLP, MBP and CNP) are shown in yellow. The occurring lipids are: cholesterol in orange, phospholipids in pink and glycosphingolipids in blue. CNP: 2'3'-cyclic-nucleotide 3'-phosphodiesterase; FMC: Fast-migrating cerebroside; GalCer: Galactosylceramide; GM<sub>1</sub>: Monosialoganglioside; GM<sub>4</sub>: Sialosyl-galactosylceramide; MAG: Myelin-associated glycoprotein; MBP: Myelin basic protein; MOG: Myelin oligodendrocyte glycoprotein; PLP: Proteolipid protein; sGalCer: Sulfatide.

Adapted from: Podbielska, Maria; Levery, Steven B.; Hogan, Edward L. 2011. The structural and functional role of myelin fast-migrating cerebroside: pathological importance in multiple sclerosis. (doi: 10.2217/clp.11.8)

## 2.1 Formation of the myelin sheath

Myelin wraps axons as a multilamellar membrane sheath. It is made by oligodendrocytes in the CNS. One oligodendrocyte can myelinate many axons (Rasband, 2015). As soon as an oligodendrocyte makes contact with an axon the synthesis is triggered. The synthesis is stimulated by a combination of factors. Then the oligodendrocytes form a cup around the axon at the point of contact. It elongates laterally and forms a trough. The two lips spread along the axon until they meet. One lip passes beneath the other one and forms the inner

tongue of the myelin sheath. The inner tongue wraps around the axon many times in order to form the multiple membrane layers (Compston, et al., 1998).

The membrane is interrupted along the course of the axon at the nodes of Ranvier, which are unmyelinated. At the nodes of Ranvier there are high concentrations of sodium channels. This results in a low electrical resistance and the depolarization is facilitated. This leads to a saltatory conduction of the action potential which is more rapid than a continuous propagation of the nerve impulse (Compston, et al., 1998).

The formation of the myelin sheath in the PNS is carried out by Schwann cells. In the PNS one Schwann cell can only myelinate one axon. However the formation in the PNS is also well-defined and depends on the interaction with some factors (Rasband, 2015).

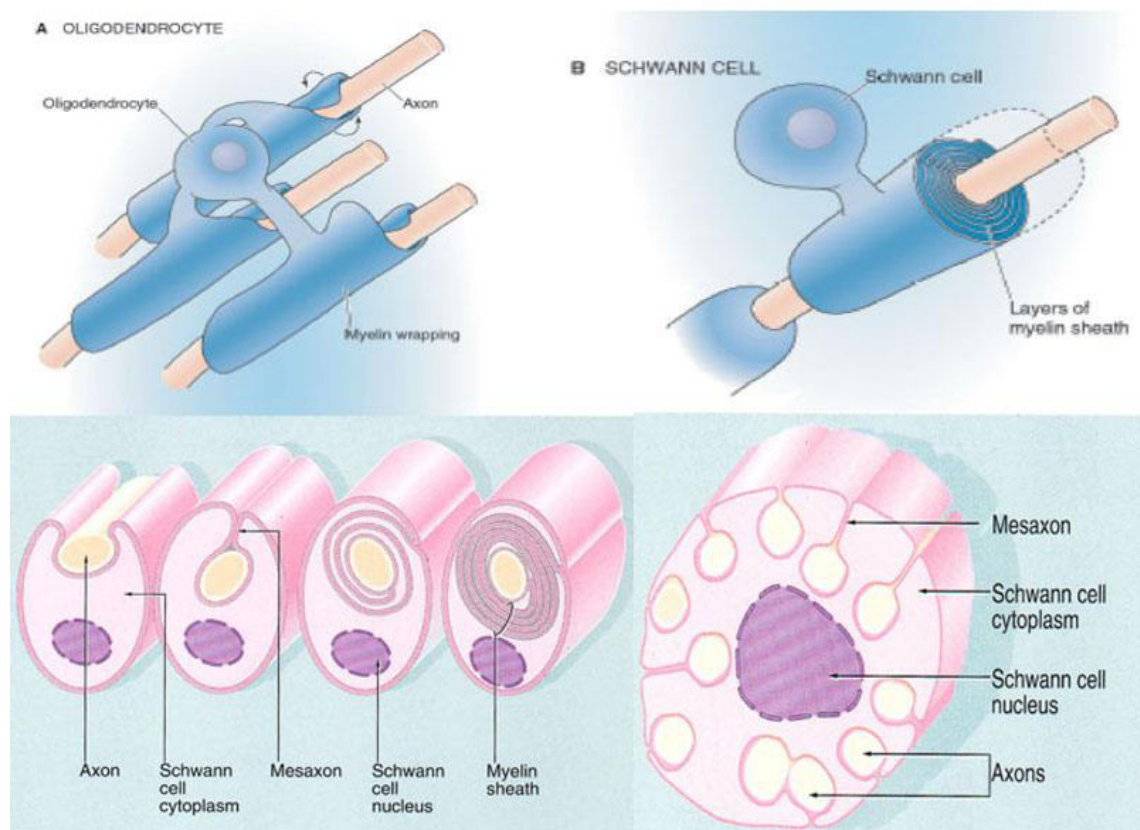


**Figure 2: Formation of the myelin sheath. (A)** The myelin sheath is formed by oligodendrocytes in the CNS. One oligodendrocyte is able to myelinate many axons. **(B)** Schwann cells form the myelin sheath in the PNS. One Schwann cell can only myelinate one axon. Obtained from: [http://medcell.med.yale.edu/systems\\_cell\\_biology\\_old/nervous\\_system.php](http://medcell.med.yale.edu/systems_cell_biology_old/nervous_system.php) (11.12.2015)

## **2.2 Proteolipid protein (PLP)**

Proteolipid protein is a major component of myelin. It differs from other components, because it is an integral membrane protein and has marked lipophilic properties (Compston, et al., 1998). PLP has a strongly conserved amino acid sequence. The sequence contains many membrane spanning domains. PLP may play a role in oligodendrocyte differentiation and therefore has a structural role in myelin formation (Siegel, et al., 1999). Moreover it stabilizes myelin membrane surfaces in compact myelin (Baron, et al., 2015). Although PLP has many important functions it is not indispensable for the composition and stability of myelin. (Siegel, et al., 1999; Nave, 2003). A knockout mouse for PLP evolves phenotypically normal and is able to get over a year old. However the stability of the myelin membrane is clearly reduced. A detailed examination of this knockout mouse showed that PLP has an impact on the longterm survival of axons in the brain and the spinal cord. Older knockout mice (>1 year) showed symptoms of a progressive axonal dysfunction (Nave, 2003).

## **2.3 Myelin basic protein (MBP)**

Myelin basic protein (MBP) is located on the cytoplasmic face of the myelin sheath (Siegel, et al., 1999). It is the major structural component of myelin and is required for normal compaction of myelin. The MBP gene has 7 exons. Due to alternative splicing of the 7 exons there are several isoforms of MBP possible. Defects in the gene or the promotor could influence the gene product or the transcription itself. This can cause abnormal myelination or failure of remyelination (Compston, et al., 1998).

Many MBP molecules have phosphate groups. The turnover rate of these groups is rapid. This post-translational modification could influence the close apposition of the cytoplasmic faces. Furthermore it is possible that this modification has a dynamic effect on the process (Siegel, et al., 1999).

Moreover this protein can be injected into an animal and leads to a cellular immune response, which results in the CNS autoimmune disease experimental allergic encephalomyelitis (EAE) (Siegel, et al., 1999).

### *2.3.1 PLP, MBP and multiple sclerosis*

In multiple sclerosis PLP and myelin basic protein (MBP) are regarded as primary targets for self-destructive T-cells (Kondo, et al., 1996). Patients who suffer from MS have a higher frequency of activated (IFN- $\gamma$ -secreting) T-cells reactive to PLP and MBP (Compston, et al., 1998; Kondo, et al., 1996). The reactivity of peripheral blood mononuclear cells to PLP in patients with relapsing or progressive MS is confined to two overlapping peptides and is associated with increased duration and disability (Compston, et al., 1998).

## **2.4 Myelin – associated glycoprotein (MAG)**

MAG is only located in the periaxonal oligodendroglial membranes of the CNS myelin sheaths. It is not present in the compact multi-lamellar myelin. MAG might be involved in important signalling mechanisms between axons and oligodendrocytes during myelin formation (Siegel, et al., 1999). However transgenic mice, which lack the gene for MAG, seem to have a normal myelination (Compston, et al., 1998). One important function of MAG is considered to be the maintenance of axon-myelin complexes (Siegel, et al., 1999).

There are two isoforms of myelin-associated glycoprotein in rodents, which are developmentally regulated. The isoforms differ in their cytoplasmic domains and are created by alternative splicing of mRNA. The isoform with the longer C-terminal tail (L-MAG) is found early in development during active myelination of the CNS. S-MAG, which has a shorter C-terminal tail than L-MAG, increases during development and is present in adult rodents (Siegel, et al., 1999).

## **2.5 2',3'-cyclic nucleotide 3'-phosphodiesterase (CNP-ase)**

CNP-ase is concentrated in specific regions of the myelin sheaths associated with the cytoplasm, for instance the oligodendroglial processes, inner and outer tongue processes and lateral loops (Siegel, et al., 1999).

The activity of CNP-ase is increased in active stages of MS, but not during remission (Compston, et al., 1998).

## **2.6 Myelin – oligodendrocyte glycoprotein (MOG)**

MOG is a transmembrane glycoprotein and is localized on the surface of myelin sheaths and oligodendrocytes. Therefore it may transmit extracellular information to the interior of the oligodendrocytes. MOG is a target antigen in autoimmune aspects of demyelinating diseases of the CNS (Siegel, et al., 1999). Furthermore it seems to be the most important target antigen for antibody-mediated demyelination (Compston, et al., 1998).

## **3. Experimental models of MS**

The pathogenesis of MS and other diseases of the CNS can be understood with the help of experimental models. It is possible to study the evolution and pathogenesis of inflammatory demyelinating lesions. Furthermore these models have contributed much to the understanding of basic aspects of neuroimmunology (Compston, et al., 1998).

A variety of experimental animal models have been used to study the pathogenesis and experimental treatment of diseases that are similar to MS. There is a variety of distinct animal models, which are defined by the animal species, the target autoantigen and the method of induction (Joy, et al., 2001). Inflammatory demyelinating lesions can be induced in experimental animal models by three different types: Experimental allergic encephalomyelitis (EAE), virus-induced demyelination (Compston, et al., 1998), toxic models of MS (Procaccini, et al., 2015) and genetically modified animals (Joy, et al., 2001).

### **3.1 Experimental allergic encephalomyelitis (EAE)**

Experimental allergic (autoimmune) encephalomyelitis (EAE) is one of the most studied experimental models in immunology. It added much to the understanding of basic T-cell immunology and the pathogenesis of inflammation (Compston, et al., 1998; Shin, et al., 2012).

EAE can be induced in almost all mammalian species (Compston, et al., 1998; Constantinescu, et al., 2011). The autoimmune syndrome can generally be induced by intradermal immunization with myelin antigens, which can be natural

or synthetic, or by adoptive transfer of T-lymphocytes reactive against myelin proteins (Joy, et al., 2001). T-lymphocytes, which are reactive against CNS proteins, are required for the induction of the disease. The transfer of T-lymphocytes from sensitized donors to naive recipients causes an autoimmune-mediated inflammation of the brain. This is possible with monospecific T-lymphocyte lines and clones as well. In most cases induction by monospecific T-lymphocyte lines results in an acute monophasic disease characterized pathologically by inflammation. In general demyelination and associated tissue damage does not occur. In contrast to the lesions of MS the inflammation is dominant and the sparse demyelination mainly happens in the perivascular CNS parenchyma. All of these pathological features are part of the acute disseminated leucoencephalomyelitis (Compston, et al., 1998; Furlan, et al., 2009).

However active sensitization with the whole CNS tissue or large components of myelin proteins leads to a prolonged chronic progressive or relapsing disease. In this case the pathological features are inflammation, widespread primary demyelination and gliosis. These models are very difficult to induce in a reproducible way and they have an unstable nature, which depends upon many different factors, for instance the mode of sensitization and the genetic background of the animal (Compston, et al., 1998; Furlan, et al., 2009). The modes of sensitization include the route of immunization, which is mostly subcutaneously, and the use of immunogens emulsified with complete Freund's adjuvant (CFA). This mixture contains *Mycobacterium tuberculosis* to create an antigen depot. Boosts with *Bordetella pertussis* are often used to assist with opening the blood-brain barrier (BBB) (Furlan, et al., 2009). Nevertheless these models resemble the pathology of MS more closely and they can be induced in many different animal species and strains (Compston, et al., 1998; Höftberger, et al., 2015).

Besides the T-cell-mediated inflammation, antibodies against myelin components are very important for the pathogenesis of chronic demyelinating variants of EAE (Compston, et al., 1998; Furlan, et al., 2009). In a variant of EAE, tissue destruction can be augmented by co transfer of anti-myelin antibodies after T-cell transfer.

Figure 3 shows the histopathology and the immunohistochemistry of a standard EAE model (MOG 1-125/CFA in DA rats). Figure 3A displays the spinal cord of the standard EAE that is stained with haematoxylin and eosin (HE). Many cellular infiltrates are visible (dark blue dots). Figure 3B shows the luxol fast blue (LFB) stained spinal cord in an adjacent slide. The pink colour of this stain shows the typical widespread demyelination, while normal unaffected myelin is shown in blue. The myelin component PLP is detected by immunohistochemistry in figure 3C. The loss of the brown signal is a marker for a widespread demyelination in the spinal cord. In this standard EAE lesions are predominantly found in the spinal cord and less frequent in the brain. If lesions are found in the brain, most are located in the periventricular areas and the cerebellum. Cortical lesions are very rarely seen, if ever.

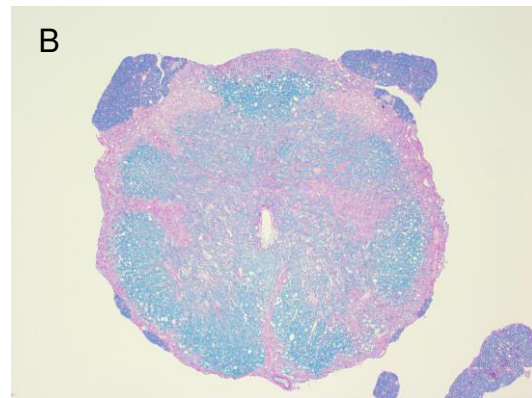






**Figure 3: Standard EAE stained with haematoxylin and eosin (HE), luxol fast blue (LFB) and PLP-immunohistochemistry (PLP-IHC).** (All pictures were taken with a 100-fold magnification) **(A)** This HE staining shows the spinal cord of a standard EAE. There are many cellular infiltrates visible. **(B)** Spinal cord of the standard EAE stained with LFB. In this picture a widespread demyelination manifests itself in the pink colour of the LFB staining. **(C)** PLP-IHC of the spinal cord of the normal EAE. The missing brown signal of the PLP-IHC can be interpreted as a widespread demyelination.

The pathogenic agents of EAE are CD4+ T-cells (Joy, et al., 2001). They recognize target autoantigen in the molecular context of major histocompatibility complex (MHC) class II proteins (Compston, et al., 1998). When they are stimulated, they produce cytokines of the proinflammatory Th1 pattern (IFN- $\gamma$  and TNF- $\alpha$ ). Precursors of CD4+ T-cells are found in the normal immune repertoire. Only the activation by antigens, microbial superantigens or mitogens can unfold their pathogenic potential (Joy, et al., 2001).

### 3.1.1 Animal strains and their characteristics

EAE can be induced in many species and strains, such as monkeys, mice, rats and guinea pigs (Constantinescu, et al., 2011; Furlan, et al., 2009). The first species where sensitization with nervous tissue accidentally led to an inflammatory demyelinating CNS disease were humans. That was due to a rare complication of rabies vaccination with virus grown on rabbit spinal cord (Constantinescu, et al., 2011). In principle EAE can be induced in all mammalian species as long as they are properly immunized. However the clinical, pathological and immunological picture of the autoimmune models of demyelination depends upon the mode of sensitization, the nature of the immunogen and genetic background of the species and strain (Furlan, et al., 2009). The EAE mod-

el can be induced by either active immunization with myelin-derived proteins or peptides in adjuvant or by passive transfer of activated myelin-specific CD4<sup>+</sup> T lymphocytes (Robinson, et al., 2014). EAE is a multifunctional animal model, but it needs to be tailored to the scientific question being asked (Constantinescu, et al., 2011). The most frequently used models are mouse models, because of the inbred genotype of laboratory mice, their rapid breeding capacity, the ease of genetic manipulation and availability of transgenic and knockout mice to facilitate mechanistic studies (Robinson, et al., 2014).

Immunization with MOG35-55 in the C57BL/6 mouse can lead to monophasic or chronic, persistent form of EAE. Multifocal, confluent areas of mononuclear inflammatory infiltration and demyelination in the peripheral white matter of the spinal cord are typical for the monophasic form. The inflammatory infiltrate mainly consists of macrophages and CD4<sup>+</sup> T-cells. The other possible form of EAE is often induced with a booster injection of the same myelin peptide 7 days after the initial immunization. It has a similar pathology with a reduced tendency to resolution of inflammation and demyelination after the peak of the disease. This animal strain and its form of the disease is a good model for chronic inflammatory demyelination, which resembles SPMS (Constantinescu, et al., 2011).

SJL/J (Swiss Jim Lambert) mice were developed by James Lambert from three different sources of Swiss Webster mice (JAX®, 2016). They display a very high incidence of reticulum cell sarcomas resembling Hodgkin's disease at the age of one year (Kumar, 1983; JAX®, 2016). This inbred strain is also characterized by extreme aggression in males and its susceptibility to EAE (Vafiadaki, et al., 2001; JAX®, 2016). SJL/J mice develop a spontaneous myopathy which results from a splice-site mutation in the dysferlin gene. As a result the level of dysferlin proteins is decreased (Weller, et al., 1997). So this strain is a good model for limb girdle muscular dystrophy 2B (Vafiadaki, et al., 2001). However the SJL/J mouse is extremely sensitive to the induction of autoantibodies and autoimmune diseases. This sensitivity could be related to the known SJL defect in those suppressor cells involved in the maintenance of tolerance and regulation erythrocyte autoantibodies (Hutchings, et al., 1986). In SJL/J mouse, EAE can

be actively induced by immunization with CNS homogenate, PLP, MBP or encephalitogenic epitopes of PLP (PLP139-151, PLP178-191), myelin oligodendrocyte protein (MOG92-106) or MBP (MBP84-104) in an emulsion with complete Freund's adjuvant (CFA) (Robinson, et al., 2014). This induces a relapsing-remitting disease. In this model the T-cell reactivity spreads to new myelin peptide determinants with each relapse, which is called epitope spreading. The form of the disease is characterized by lesions in the optic nerve, brainstem, spinal cord, cerebellum and cerebral cortex. At first there is perivascular and meningeal lymphocyte and neutrophil infiltration. Then the inflammatory infiltration is resolved and there is a progression of white matter damage and gliosis, demyelinated axons and myelin debris, which contains macrophages (Constantinescu, et al., 2011).

The Lewis rat was developed by Dr Lewis from Wistar stock in the early 1950s. This strain is characterized by an albino colouring, low fertility and a docile behaviour (Charles, 2016). However the lifespan of the Lewis rat is basically determined by the occurrence of spontaneous neoplasms. The highest incidences were observed for adenomas of the pituitary gland and adenomas/adenocarcinomas of the adrenal cortex in both sexes, mammary gland tumours and endometrial carcinomas in females, and C-cell adenomas/adenocarcinomas of the thyroid gland and tumours of the haemopoietic system in males (Baum, et al., 1995). This strain is used for transplantation research, induced arthritis/inflammation, EAE, streptozotocin (STZ)-induced diabetes (Charles, 2016). Active EAE can be induced by MBP. Passive EAE results from the transfer of MBP-specific T-cells in the Lewis rat. It causes severe CNS inflammation with hardly any demyelination. So this serves as a good model for the investigation of acute CNS inflammation. Moreover an injection with anti-myelin antibodies, for instance MOG antibodies, induces demyelination and increased perivascular inflammation and clinical symptoms; after that remyelination occurs (Constantinescu, et al., 2011).

The Dark Agouti inbred model was developed by the Agricultural Research Council Institute of Animal Physiology at Cambridge. About 30-40% of the population develops a white belly spot of the size of a quarter. This phenotypic

trait is inherited in a non-Mendelian fashion. It is present in females and males and has incomplete penetrance. There is a high incidence of bladder tumours in males and hormone-dependent endometrial adenocarcinoma in females. This strain is widely used in transplantation studies and is susceptible to experimentally induced arthritis, EAE and induction of autoimmune thyroiditis (Taconic, 2016). EAE in the Dark Agouti (DA) rat can be induced by syngeneic spinal cord tissue or recombinant rat-MOG. Demyelination and spinal cord lesions with perivascular and subpial inflammatory infiltration are specific for this form of EAE (Constantinescu, et al., 2011). This model resembles many histological features of multiple sclerosis, though not all.

### *3.1.2 Differences between MS and EAE*

Experimental animal models of MS are based on the use of rodents, mostly rats and mice. The rodent and human immune systems are different. So not all observations made in rodent EAE can be directly translated to human MS (Joy, et al., 2001).

A major difference between MS and EAE is that EAE requires an external immunization step to develop. In humans the sensitization to autoantigens is not artificially induced. The inducing antigens are known in EAE, while so far in MS there is no unique identified antigen. The different methods of priming and activating autoreactive T-cells could be the reason for the differences between these conditions (Constantinescu, et al., 2011).

Furthermore EAE is generally affecting the spinal cord white matter. In contrast MS is mainly a brain disease with demyelination of the cerebral and cerebellar white matter and cortex. Unfortunately there are hardly any cortical lesions in EAE. So there are only a few studies that were able to investigate cortical lesions in EAE. (Procaccini, et al., 2015).

Another disadvantage of these animal models is that they do not necessarily mirror the cellular or molecular pathology of MS. On the one hand some types of EAE produce brisk demyelination. On the other hand other types only lead to a minor demyelination. It is difficult to say which model is the best. Yet the fea-

tures of MS are not fully understood. Therefore it is very challenging to know how faithfully any animal model of MS resembles the human disease (Joy, et al., 2001).

### **3.2 Virus – induced inflammatory demyelinating diseases**

There are many possibilities for a virus to cause demyelination. Viruses can directly lyse oligodendrocytes, which produce the myelin. In other cases the immune system and its reaction against the virus is involved (Joy, et al., 2001). The major problem of these models is their pathogenetic complexity. The virus must be neurotrophic in order to produce an inflammatory and demyelinating lesion. Furthermore the virus has to persist in the CNS and trigger a pathogenic anti-viral immune response. The immune response is complex. It involves the cellular and the humoral immune mechanisms (Compston, et al., 1998). However the mechanism of the virus-induced immune-mediated demyelination is not clear yet (Joy, et al., 2001).

Theiler's murine encephalomyelitis virus (TMEV) and the mouse hepatitis virus (MHV) are the most developed models (Joy, et al., 2001).

#### *3.2.1 Theiler's murine encephalomyelitis virus (TMEV)*

TMEV belongs to the family of *Picornaviridae*. This virus strain is divided into two subgroups. The GDVII subgroup strain leads to an acute fatal polioencephalomyelitis in mice. There is no virus persistence or demyelination. The TO subgroup strain induces a milder polioencephalomyelitis that is followed by virus persistence and demyelination (Takano-Maruyama, et al., 2006).

The DA strain, which is a representative strain of the TO subgroup (Takano-Maruyama, et al., 2006), leads to an inflammatory demyelinating disease of the spinal cord. The lesions are similar to lesions of MS. Demyelination is supported by the immune system. T cells directed against viral antigens are partly responsible for inflammatory, demyelinating and multi-focal lesions (Joy, et al., 2001).

The genome of TMEV is simple. There is plenty of detailed structural information of the virus. This model can easily be genetically manipulated and there is much knowledge of the genes and immune system of the natural host,

the mouse. However the pathogenesis of the demyelinating disease is not completely understood. On the one hand there has to be virus persistence in oligodendrocytes and microglia to get a TMEV-induced demyelination. On the other hand the immune system assists in the late demyelinating disease, but the exact mechanism are still poorly understood (Joy, et al., 2001).

### 3.2.2 *Mouse hepatitis virus (MHV)*

There are many different strains of the mouse hepatitis virus (MHV) that can cause a variety of diseases, for instance hepatitis, respiratory and CNS disorders. JHM, S and A59 strains of MHV induce demyelination (Joy, et al., 2001).

Intracranial inoculation of mice with the JHM strain of MHV leads to the distribution of viral particles throughout the ventricular system. It is targeting ependymal cells lining the ventricles. Then the virus penetrates into the parenchyma of the brain and spinal cord. Oligodendrocytes, astrocytes and microglia are more likely to be infected. The JHM infection is followed by an innate host-defence response that is characterized by the secretion of proinflammatory factors including TNF- $\alpha$ , IFN- $\alpha$ , IFN- $\beta$ , IL-1, IL-6 and IL-12. Moreover neutrophils, macrophages and natural killer cells respond to the JHM infection. They migrate to the CNS to assist in permeabilizing the blood brain barrier (BBB) (Marro, et al., 2014).

The extent of demyelination depends on the genotype of the virus, dosage and the route of inoculation. The strain, age and immune status of the infected mouse plays an important role too. Furthermore MHV has a large viral genome, making it a complex pathogen. A system for fast and efficient mutagenesis has not been fully developed (Joy, et al., 2001).

### 3.3 Toxic models of MS

Toxic demyelination is used to study the process of de- and remyelination. The two most common agents to induce demyelination are cuprizone and lysolecithin (Procaccini, et al., 2015).

Cuprizone (bis-cyclohexanone-oxaldihydrazone) is a copper chelating reagent. It is added to the normal rodent food. Cuprizone leads to oligodendroglial cell

death with subsequent demyelination and it causes a profound activation of astrocytes and microglia. The specific targets of cuprizone are mature oligodendrocytes. They undergo apoptosis because they cannot meet the metabolic demand. Oligodendrocytes have a copper deficiency due to the copper chelate characteristics of cuprizone. That is the main reason for the metabolic failure. However other cell types are not affected. As soon as the cuprizone is removed from the diet and the demyelination is complete, new oligodendrocytes which are generated from a pool of oligodendrocytes progenitors (OPC) begin to form new myelin sheaths. When cuprizone is added to the food continuously, the remyelination is abortive and demyelination persists until the end of the diet. The result is a chronic demyelination. After the removal of cuprizone from the diet, the remyelination capacity retains but is strongly decreased (Procaccini, et al., 2015).

Lysolecithin, another substance causing toxic demyelination, is an activator of phospholipase A2. It is injected into the spinal cord in several animals, such as cats, rabbits, rats and mice. It induces focal areas of demyelination. Lysolecithin has primary toxic effects on myelin sheaths and causes a highly reproducible form of demyelination in the CNS. It does not damage adjacent cells and axons. Moreover it is not immune-mediated. It even takes place in immune-deficient mice. If young animals are used there is hardly any chronic inflammation in lesions and a complete remyelination takes place in 5-6 weeks. Older animals experience a slower repair. T cells, B cells, macrophages and neutrophils are infiltrating the lesion sites in the acute phase, which is directly after the lysolecithin injection. T-cell response enhances the expression of different neurotrophins by macrophages and astrocytes that sustain neuronal protection and survival. Many growth factors are produced during the remyelination process. T cells stimulate the activity of the CNS glia, thus supporting the remyelination of oligodendrocytes (Procaccini, et al., 2015).

### **3.4 Limitations of animal models in MS**

MS is a multifaceted disorder. There is no single experimental model representing the entire complexity of this human disease. To date, EAE is the most wide-

ly accepted animal model of MS as it comes in numerous, distinct variants, which may reflect individual aspects of MS (Wekerle, 2008; Mix, et al., 2010).

Nevertheless there are some limitations to the use of this animal model, since there are differences in the pathogenesis of EAE compared to that of MS. The EAE model provides very few information about MS progression and allows no detailed study of relapse rates. It is also very difficult to examine remyelination in EAE. Lesions occur stochastically with regard to timing and localization (Procaccini, et al., 2015), but most often in the lower spinal cord white matter.

Furthermore this animal model may not be suitable for screening of new treatments (Mix, et al., 2010). Studies that were trying to evaluate the potential benefits of novel therapeutic treatments with neuronal growth and survival factors were unsatisfactory. Many effects were off-target. This makes any results difficult to interpret (Procaccini, et al., 2015).

In MS demyelination is also not restricted to perivenous regions of the white matter. An extensive demyelination of the cerebral cortex in the absence of inflammation is common in MS which is not seen in EAE (Sriram, et al., 2005). There is an association between cortical lesion load and both physical and cognitive disability in patients with MS (Calabrese, et al., 2012, Geisseler, et al., 2016). Previous studies have shown that the accumulation of cortical lesions is associated with the development of a higher degree of disability in relapsing remitting and secondary progressive multiple sclerosis (Calabrese, et al., 2012). However the pathogenesis of cortical lesions in human MS is largely unknown. This could be due to the lack of useful animal models which are reflecting the human cortical pathology. Moreover the fact that rodent EAE rarely affects the brain is another obstacle (Merkler, et al., 2006).

#### **4. Aim of this thesis: Generating a new model involving cortical lesions with close resemblance to human MS**

Rodent animal models as described in the previous chapter mimic many, though not all histological features of MS. In the currently available spectrum of



available models however there is none that shows a predictable and stable occurrence of cortical lesions. Cortical lesions differ to white matter lesions histologically in a relative lack of cellular infiltrates.

The aim of this thesis is to produce a targeted inflammatory demyelinating lesion in the neocortex of the rat by an implanted catheter. Serial MRI scans and subsequent histological analysis will depict the lesion development. We develop an animal model that features constant cortical lesions in the neocortex and enables us to access the lesions in the living rat.

## **5. Material and methods**

### **5.1 Animals**

For the experiments adult male Dark Agouti (DA) rats were used. This strain is often used for immunopharmacological studies. In 1997 Kamada et al showed that DA rats are more susceptible to immunological phenomena than other rat strains. The animals were obtained from Harlan, Netherlands. We used male animals because we wanted to achieve standardization. In contrast female rats have hormonal variations, which could affect the immune system.

### **5.2 Catheter implantation**

A schema of the rat brain is shown in figure 4. Compared to the human brain the rat brain has less white matter, which is in the rat mainly concentrated in the Corpus callosum.

The catheter was placed into the right cerebral hemisphere according to the following coordinates – 2mm posterior to the bregma, 2,4mm lateral to the median, 2mm depth. The catheter was obtained from PlasticsOne, Roanoke, VA, USA.

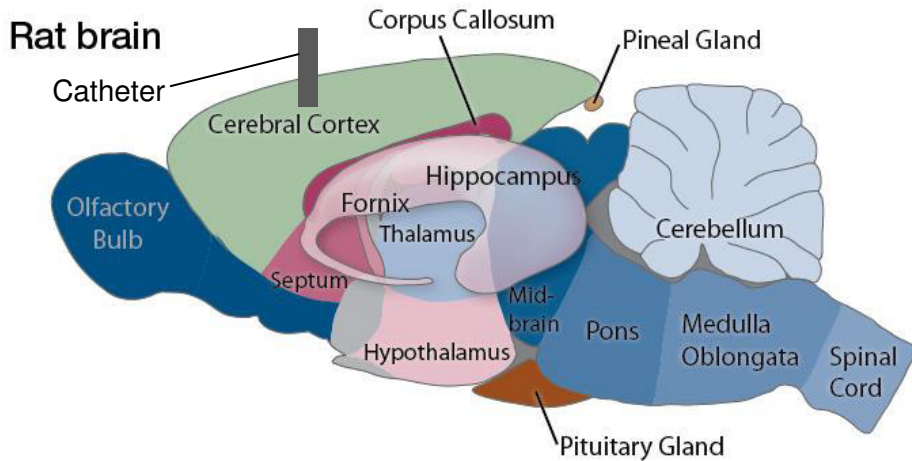


**Figure 4: Schema of the rat brain.** The grey bar illustrates the placement of the catheter. Adapted from: <http://learn.genetics.utah.edu/content/addiction/mice/> (11.12.2015)

### 5.3 Immunization procedure

Immunization was done 2 weeks after implantation to allow proper wound healing. The animals were briefly anaesthetized by isoflurane and injected subcutaneously at the base of the tail with a total volume of 200  $\mu$ L MOG 1-125 emulsion (10  $\mu$ g per animal). To prepare this emulsion MOG was dissolved in phosphate buffered saline (PBS) and then emulsified in incomplete Freund's adjuvant.

### 5.4 Enzyme-linked immunosorbent assay (ELISA)

After 4 weeks a blood sample was drawn from each animal and the serum titers of anti-MOG antibodies were determined by ELISA analysis according to standard protocols. In short, MOG (5  $\mu$ L MOG/mL PBS) was coated on a 96 well plate and incubated for 1h at 37°C. Then the plate was blocked with 1% bovine serum albumin (BSA) in PBS for 1h at room temperature. Afterwards the plate was incubated with rat sera (1:50) and standard for 2h at 37°C. IgG specific horseradish conjugated anti-rat antibody (1:10 000) was used for detection. 2,2'-Azino-bis(3-ethylbenzthiazoline-6-sulfonic acid) (ABTS) was added as substrate. Between these steps the plate was washed three times with PBS/Tween. The optical density was measured at 405nm.

## **5.5 Opening of the blood brain barrier (BBB)**

Once a sufficient antibody titer was achieved, the sensitized rats were again briefly anaesthetized with isoflurane. Then a mixture of inflammatory cytokines was injected with the help of the implanted catheter. We used 150 U of interferon- $\gamma$  and 250 ng of tumor necrosis factor- $\alpha$  in a total volume of 2500  $\mu$ L. Therefore the cytokines were mixed with PBS. A total volume of 2  $\mu$ L was injected per rat.

Several MRI scans were performed on the rats at day 6, 10 and 13 after the opening of the BBB.

Animals were observed daily for the development of any signs of illness.

## **5.6 Magnetic Resonance Imaging (MRI)**

MRI is based on the phenomenon that atomic nuclei with an uneven number of protons or neutrons have a nuclear spin. Carbon, sodium, phosphorus, helium and hydrogen are among these atoms. The positive charged part of the nucleus is able to rotate and creates a small bar magnetic field. The MRI scanner creates a strong permanent magnetic field, where the proton-magnetic fields arrange themselves. They can be parallel or antiparallel ordered towards the external magnetic field. The oriented protons make a precession movement around the axis of the external magnetic field. The speed of the precession is declared as frequency (Larmor frequency). The stronger the external magnetic field, the higher the Larmor frequency. The rotation speed also depends on the type of the atomic nucleus. In order to measure a signal, the oriented protons are excited with a very short high-frequency pulse. This pulse has to match the Larmor frequency, so the protons can absorb and release energy. The absorbed energy has the effect that some protons are tilting over to the energy-rich state (antiparallel towards the main magnetic field) and the rotation movement is synchronised between the protons. After the high-frequency pulse the protons release the energy as high-frequency signal. This signal is recorded by a receiver coil (Hermeij, et al., 2010).

There are differences between several tissue types. They differ in the time span that is needed until the protons are back in their initial state (after the high-frequency pulse). The  $T_1$  time is a time constant, which describes the time that is needed until the longitudinal initial state is restored and how fast the absorbed energy is released to the tissue. The  $T_2$  time describes the needed time to restore the transversal initial state. This time constant depends on the interaction between the spins (Hermey, et al., 2010).

#### *5.6.1 Animals anaesthesia during MRI scans*

The rats were anaesthetized by isoflurane inhalation. Then a mixture of fentanyl, midazolam and domitor (FMD) with a ratio of 2:2:1 was injected. The MRI scan was performed with a 16ch wrist coil. After the measurements were finished the animals received a mixture of Anexate, Antisedan, NaCl antidote (AAN, in a ratio of 8:1:3) to counteract the sedation.

### **5.7 Histopathology**

The animals were sacrificed and perfused transcardially with 4% paraformaldehyde in 0.1 M PBS between day 9 and 16 after BBB opening. Brains and spinal cords were dissected and then postfixed in the same fixative for 24h at 4°C. After washing in PBS the tissue was embedded in paraffin according to standard histological procedures. The tissue was cut into 1.5-2  $\mu\text{m}$  paraffin sections. The sections were stained with haematoxylin and eosin (HE) and Luxol fast blue (LFB).

#### *5.7.1 Fixation*

In the past years many fixation methods have been developed and optimized. This process is still viewed as a critical step; nevertheless there are some methods that are capable of keeping the epitopes (Luttmann, et al., 2014).

In our study the tissue was fixed in 4% paraformaldehyde/PBS solution. After perfusion the tissue was kept in this solution for 24h. Then the tissue was em-

bedded in paraffin with the Thermo Shandon Citadel 1000 and the following program:

1. 50% ethanol for 30 minutes
2. 70% ethanol for 60 minutes
3. 70 % ethanol for 90 minutes
4. 80% ethanol for 60 minutes
5. 80% ethanol for 90 minutes
6. 96% ethanol for 60 minutes
7. 96% ethanol for 90 minutes
8. 96% ethanol for 120 minutes
9. Xylene for 30 minutes
10. Xylene for 60 minutes
11. 2 times paraffin for 120 minutes each

#### 5.7.2 *Haematoxylin and eosin (HE)*

HE is mainly used for nuclear stains. The chromatin pattern is shown in a distinct blue/black colour. Haematoxylin requires oxidation to haematein to be active as a basic dye (when it is combined with a mordant). Eosin is the counterpart of haematoxylin and is an acid dye. Eosin stains cytoplasm, erythrocytes, muscle and collagen. It depends on the density of these basic elements how intense the achieved colour is. The colour range is from deep red to pale pink (Orchard, et al., 2012).

#### **HE staining protocol:**

1. Deparaffinise paraffin embedded tissue sections to distilled water:
  - a. Incubate the slides for 10 min in xylene (2 times)

- b. Rinse with 96% ethanol
  - c. Rinse with 70% ethanol
  - d. Rinse with 50% ethanol
  - e. Rinse in distilled water
2. Incubate sections in filtered haematoxylin for 5 min
  3. Rinse in tap water (2 times)
  4. Differentiate in HCl-alcohol
  5. Rinse in distilled water (2 times)
  6. Incubate slides in bluing reagent (Shandon) for 5min
  7. Rinse in distilled water
  8. Dehydration through graded ethanol line
  9. Apply mounting medium and coverslip

### 5.7.3 *Luxol fast blue (LFB)*

LFB is a phthalocyanine dye that is soluble in alcohol. This dye shows a strong affinity to bases found in the lipoproteins of the myelin sheath. For this staining method the sections are normally treated with LFB over an extended period of time and then differentiation with a lithium carbonate solution is followed. As a result myelin is stained blue against a colourless background (Humphrey, et al., 2008).

#### **LFB staining protocol:**

##### Solutions:

**Luxol fast blue solution:** 1 g Luxol fast blue in 1000 mL 96% ethanol

**Perjodic acid solution:** 4 g perjodic acid in 500 mL distilled water

**Lithiumcarbonate solution:** 1 g lithiumcarbonate in 1000 mL distilled water

1. Deparaffinise paraffin embedded tissue sections to 96% ethanol:
  - a. Incubate the slides for 10 min in xylene (2 times)
  - b. Rinse with 96% ethanol
2. Incubate the sections in LFB solution at 56°C overnight (make sure the sections are fully covered with the solution)
3. Rinse with 96% ethanol
4. Rinse in distilled water
5. Incubate the slides in lithium carbonate solution for 5 min
6. Differentiate with 70% ethanol until myelin sheaths appear blue
7. Rinse in distilled water
8. Incubate the slides in periodic acid for 10min
9. Rinse in distilled water
10. Incubate the slides in Schiff's reagent for 20 min
11. Rinse the slides in warm tap water for 10 min
12. Dehydrate the tissue through a graded ethanol line
13. Apply mounting medium and coverslip

## **5.8 Immunohistochemistry (IHC)**

IHC is a method to detect relevant proteins in a tissue section by using an antibody. The task of the antibody is to localize specific antigens through binding specifically to it. The antibody is labelled with a marker, such as fluorescent dye or an enzyme to make detection possible. The aim of each IHC is to maximize the signal to noise ratio. There are different methods for detection available:

either the primary antibody is labelled directly or a second (secondary) antibody that binds to the first antibody is labelled (Luttmann, et al., 2014). In the latter case the signal is usually enhanced.

#### *5.8.1 Epitope/Antigen retrieval*

The proteins are degenerated due to the fixation step the in paraformaldehyde solution. They can be cross linked and/or coagulated. The epitope/antigen retrieval is necessary to undo this linkage so more antigens are again available for detection. The antigen retrieval is carried out by an (humid) impact of heat using microwaves, water baths, autoclaves or steamers. It is even possible to use proteolytic enzymes (Luttmann, et al., 2014).

For our study the sections were steamed in citrate (pH 6) for 1 hour in a commercially available food steamer.

#### *5.8.2 Blocking*

Unspecific binding sites cause a false positive signal. Therefore these binding sites have to be blocked. We used 10% fetal calf serum in DAKO antibody diluent to get rid of the background staining.

Background staining can also be the result of endogenous enzymes such as the endogenous peroxidase. So the sections are pre-treated with hydrogen peroxide after the deparaffinising step to avoid this kind of background staining.

#### *5.8.3 Avidin-biotin complex (ABC) and labelled avidin-biotin method:*

Biotin is a very small molecule (0,24 kDa). It is specifically bound by avidin. Avidin is a rather big molecule with a molecular weight of 68 kDa. It has four binding sites for the biotin molecule and it can be labelled with common enzymes such as peroxidase. Both methods need three steps in order to achieve a signal. First the primary unlabelled antibody binds to its antigen on the tissue section. Then the secondary antibody binds the primary one. At the third step the complex, which carries the enzyme, binds to the secondary antibody. In case of



the ABC method it is an avidin-biotin complex with an enzyme. Using the LAB method the complex consists of enzyme-labelled avidin. Afterwards the visualization step follows. The colourless and chromogen substrate is catalysed by the enzyme. As a result a coloured precipitate shows the localisation of the primary antibody and its bound antigen (Luttmann, et al., 2014). There are many other possible detection methods; however it is very easy to achieve signal amplification with the LAB method. The PLP-IHC was detected with the LAB method. A scheme of this method is shown in figure 5.

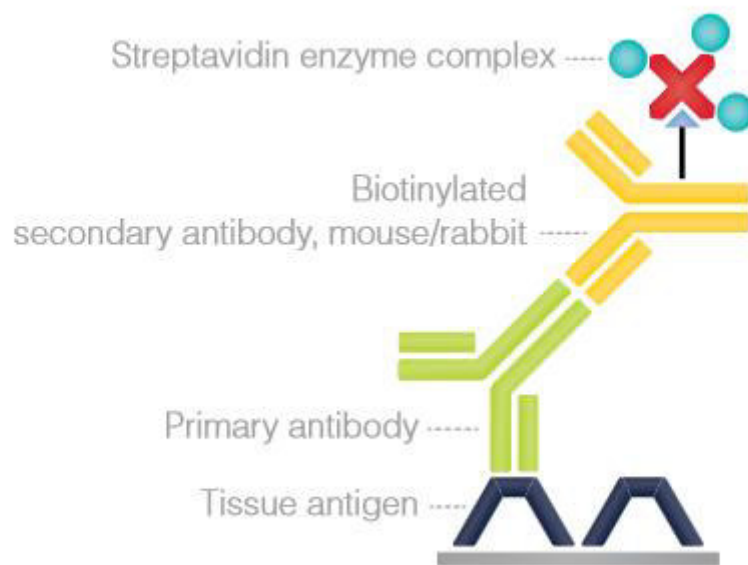


**Figure 5: Labeled (strept-)avidin-biotin (L(S)AB) method.** The tissue antigen (shown in dark blue) is specifically bound by the unlabelled primary antibody (green). The secondary antibody has to be biotinylated and binds to the primary antibody. Biotin (blue triangle) binds avidin (red) with a high affinity. Avidin is labelled with an enzyme (light blue spheres). In this study horseradish peroxidase (HRP) was used as an enzyme. It is responsible for the visualisation step. Obtained from: <http://www.dako.com/at/ihc-guidebook-detection-methods-chapter6.pdf> (11.12.2015)

#### 5.8.4 IHC staining protocol

Here we show the staining protocol for detection of the myelin protein PLP as an example. Of course the protocol has to be adjusted to fit any given antibody and give the best specific staining result.

1. Deparaffinising of paraffin embedded tissue sections:

- a. Incubate sections for 10 min in xylene (2 times)
  - b. Rinse the sections with 96% ethanol for (2 times)
  - c. Incubate for 30 min in H<sub>2</sub>O<sub>2</sub>-Methanol (180 ml Methanol + 1.2 mL H<sub>2</sub>O<sub>2</sub>)
  - d. Rinse with 96% ethanol
  - e. Rinse with 70% ethanol
  - f. Rinse with 50% ethanol
  - g. Rinse with deionized water
2. Pre-treatment: steam the sections in citric acid buffer (pH 6.0) for 1h
  3. Wash the slides 3 times in PBS
  4. Bordering the tissue with DAKO-Pen
  5. Blocking: 20 min in 10% fetal calf serum in DAKO diluent (FCS/DAKO)
  6. Get rid of the blocking solution by tipping the slide-side gently against pulp
  7. Apply primary antibody: PLP (monoclonal mouse anti PLP antibody) 1:500 diluted in FCS/DAKO. Incubate at 4°C overnight
  8. Wash 3 times in PBS
  9. Apply secondary (biotinylated anti-mouse) antibody 1:200 diluted in FCS/DAKO and incubate at room temperature for 60 min.
  10. Wash 3 times in PBS
  11. Apply avidin peroxidase labelled 1:100 diluted in FCS/DAKO and incubate at room temperature for 60 min
  12. Get rid of the avidin solution by tipping the slide-side gently against pulp

13. Visualization of the labelling with diaminobenzidine (DAB) – 2 mL DAB-Solution (1 g DAB in 40 mL PBS) in 100 mL PBS + 33  $\mu$ L H<sub>2</sub>O<sub>2</sub>, filtered
14. Stop the reaction with tap water
15. Counterstain with haematoxylin:
  - a. Incubate sections for 1 min in filtered haematoxylin
  - b. Rinse in tap water 2 times
  - c. Differentiate in 70% ethanol
  - d. Rinse in distilled water 2 times
  - e. Incubate slides for 5 min in bluing reagent
  - f. Rinse in distilled water
  - g. Dehydration through graded ethanol line
16. Apply mounting medium and coverslip

## **6. Results**

### **6.1 The catheter itself does not cause any adverse tissue reaction**

As a first step we needed to make sure that the catheter system used does not by itself cause any adverse tissue reaction even on long term implantation. Therefore, 5 animals were implanted with the catheter at the coordinates - 2mm posterior to the bregma, 2,4mm lateral to the median, 2mm depth and the animals sacrificed after 4 weeks. The brains were removed and histologically analysed for any signs of adverse tissue reaction. Previous experiments showed that after 14 days after the implantation until the BBB is fully restored (data not shown).

We found no tissue reaction near the implantation site (as shown in figure 6 and 7) even after an implantation time of 4 weeks. Figure 6 A shows the implantation site after 4 weeks after implantation in an standard HE staining, 6 B in luxol fast blue staining. The tissue appears histologically intact with no signs of e.g, pressure related local demyelination.

This is furthermore confirmed by immunohistochemistry for the myelin component PLP, as shown in Figure 7. Please note that physiologically the myelin architecture differs in density in different parts of the cortex.

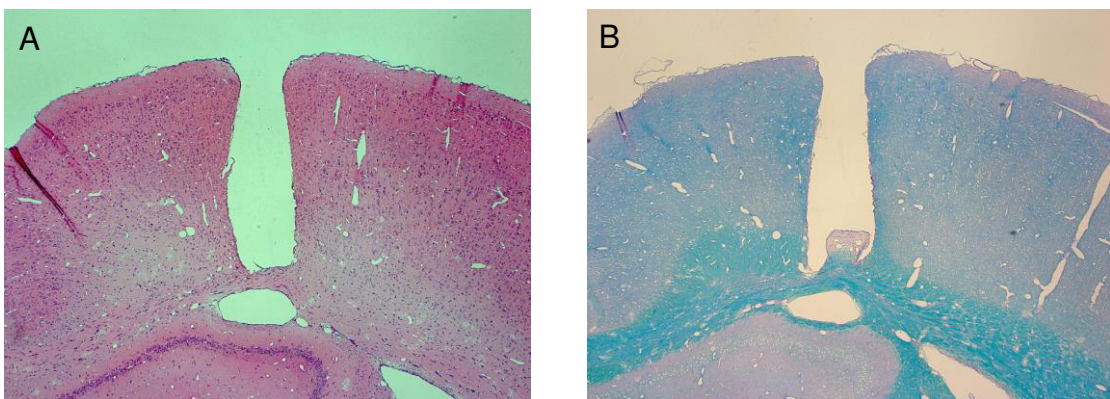


**Figure 6: HE and LFB staining of rat brain. (A)** HE staining of the rat brain tissue. There are no signs of any tissue reaction near the implanted catheter. (Magnification: x50) **(B)** LFB staining of the rat tissue. LFB is usually used to stain myelin. In this case demyelination, around the implanted catheter, does not occur. The animal was sacrificed 4 weeks after the implantation. (Magnification: x50)



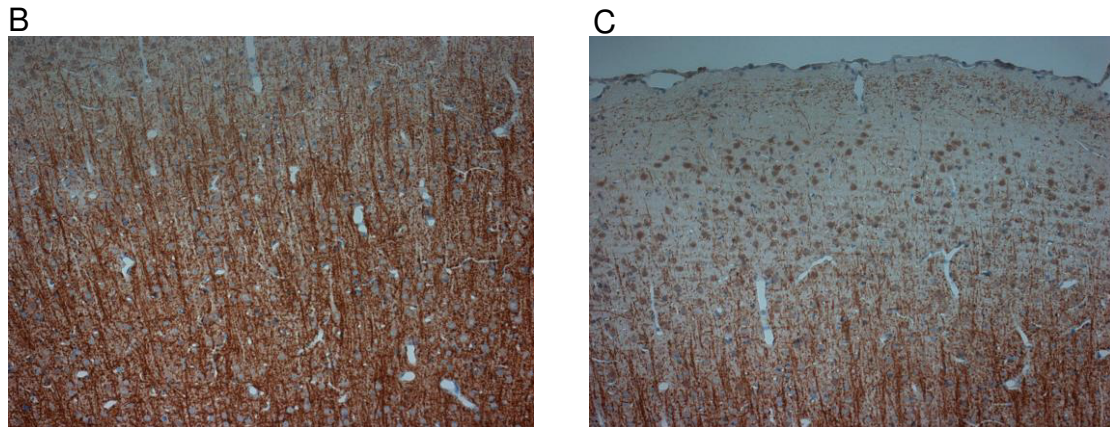


**Figure 7: PLP-IHC of the rat brain.** (A) PLP-IHC was performed on this rat brain tissue. The rat was sacrificed after 4 weeks after catheter implantation. PLP is detectable around the catheter channel in a normal density. (Magnification: x50) (B) Detailed view of the “lower” part of the rat cortex. (Magnification: x200) (C) Detailed view of the “upper” part of the rat cortex. (Magnification: x200). Please note the physiological differences in myelin density in the cortex area.

## 6.2 Clinical signs and symptoms of the animals

After cytokine injection we noticed a diffuse slowing of the animals from day 9-day 15 without any motor signs like pareses, as it is often the case in conventional EAE models. A noticeable loss of weight of up to 10 % was also detected in some of the animals, but was not found in general.

In two animals we had a more severe reaction with breathing difficulties on day 9, which lead to immediate sacrifice of these animals. Even in these animals no motor symptoms were detectable.

## 6.3 Serial MRI scans

Before (baseline scans) and after the opening of the BBB we performed serial MRI scans on the rats. The measurement time was limited to 30 minutes for one MRI scan in order of not endangering the rat’s life. The figures 8-11 are showing the T<sub>2</sub>-weighted images of the rat brain at baseline and day 6, 10 and 13. At day 6 (figure 9) we were able to detect an edema formation in the catheter region in one animal, but not in the remaining animals. However even in this animal, the edema resolved after day 6 and was no longer detectable in subsequent scans on day 10 or on day 13.



The following MRI scans are by courtesy of Prof Stefan Ropele and Johannes Strasser of Medical University Graz.

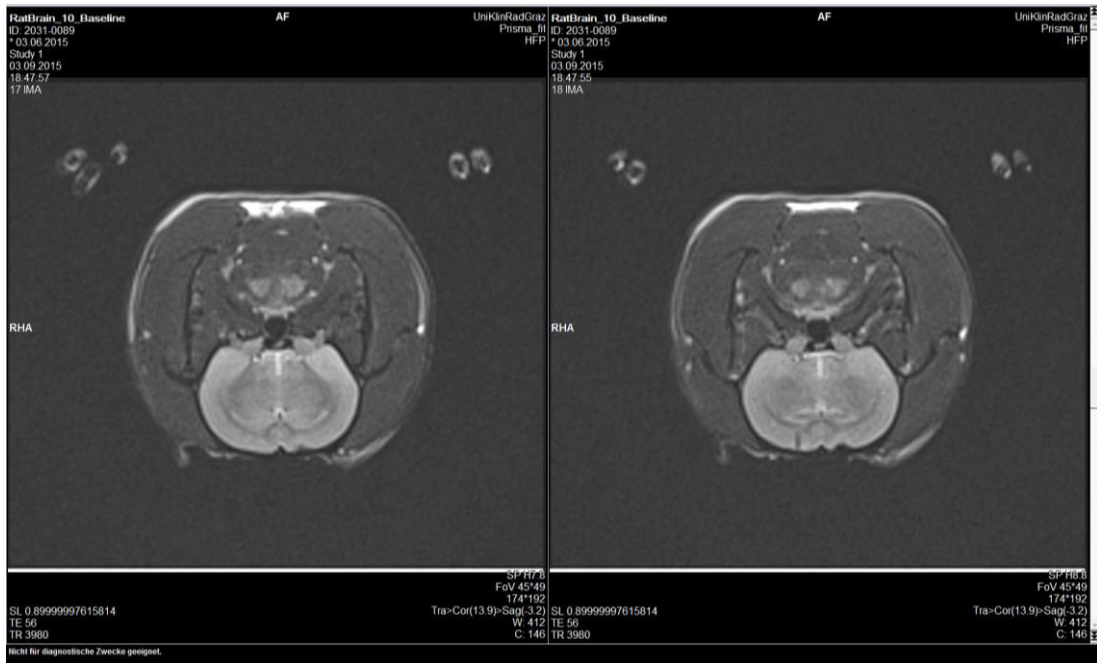


**Figure 8:**  $T_2$ -weighted baseline of the rat brain. This image shows the frames 17 and 18. In frame 18 the channel of the implanted catheter is visible.

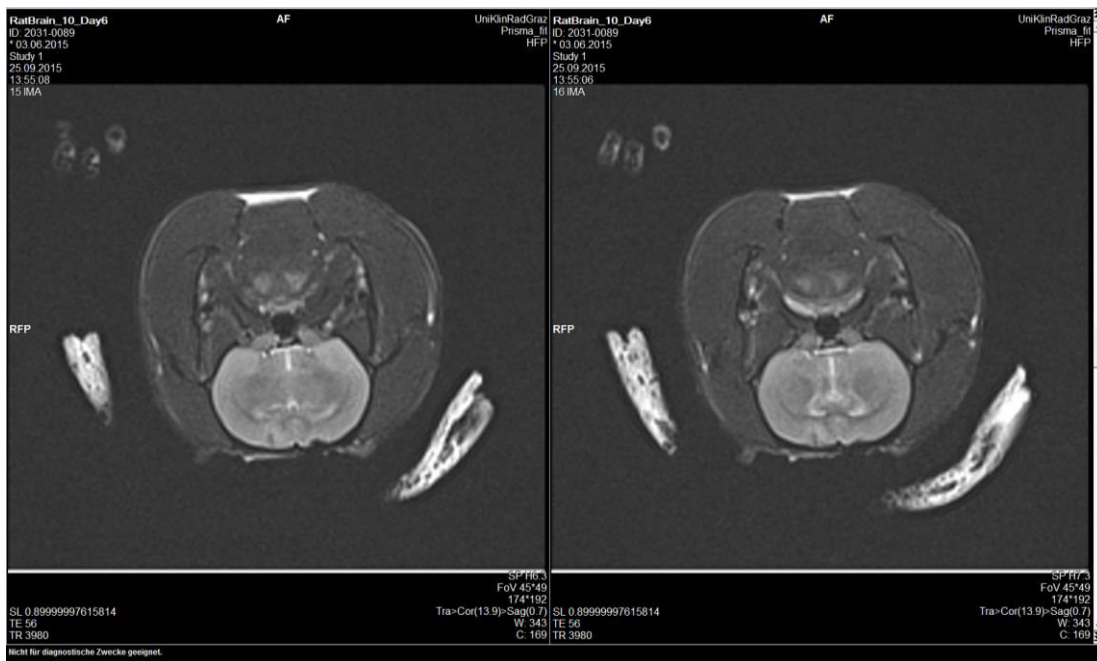


**Figure 9:**  $T_2$ -weighted MRI scan of the rat brain at day 6. This image shows the frames 15 and 16, where the channel of the implanted catheter is visible. At day 6 we were able to detect an edema at the region of the cortex in this rat brain.

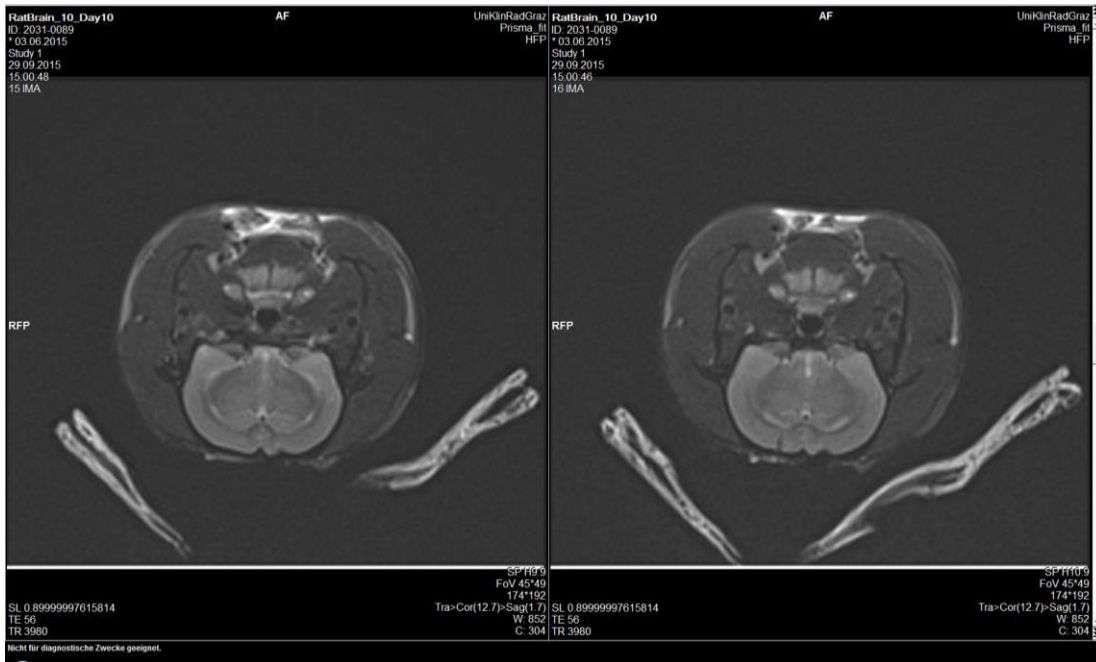


**Figure 10:**  $T_2$ -weighted MRI scan of the rat brain at day 10. The frames 15 and 16 are shown. The channel of the implanted catheter is visible in frame 16. Cortical lesions were not detectable.

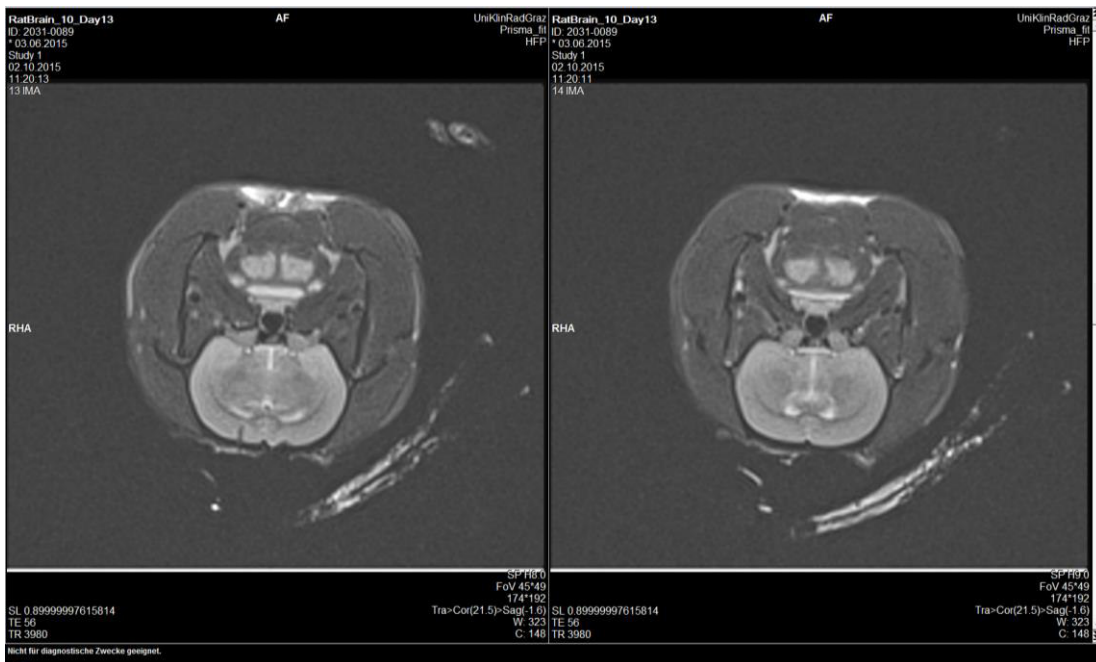


**Figure 11:**  $T_2$ -weighted MRI scan of the rat brain at day 13. This image shows the frames 13 and 14. At day 13 there are no signs of cortical lesions visible.

#### 6.4 Histopathology and immunohistochemistry shows a widespread demyelination of the cortex

Although the MRI scans were less than promising, we found a widespread demyelination in the cortex of all animals examined. Figure 12 shows cortical areas of the same rat shown in the MRI scans above (sacrificed on day 16 after opening of the blood brain barrier) in luxol fast blue staining (LFB). The overview of the demyelination in the cortex is shown in figure 12 A (100x). A detailed view of the demyelinated cortex is shown in figure 12 B at 200x magnification. The demyelination is not only found in direct vicinity of the catheter implantation site, but extends over the contralateral hemisphere as well.

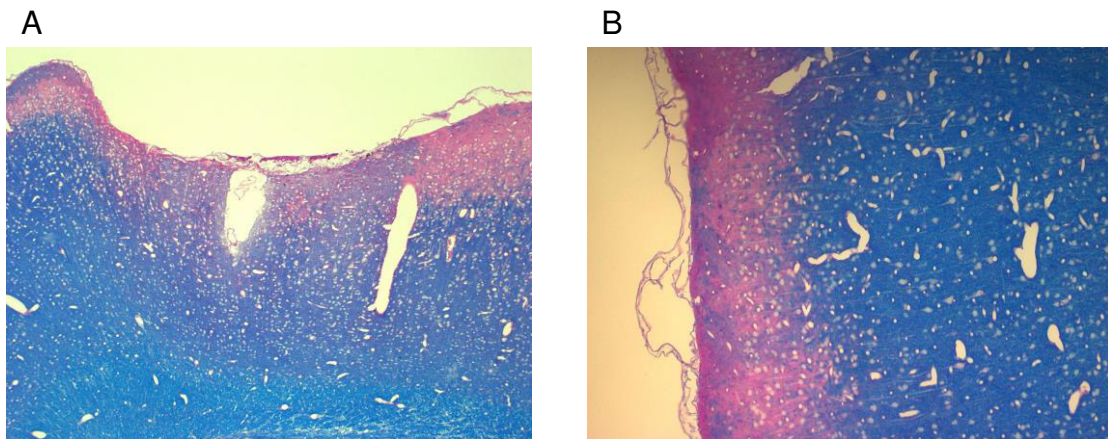


**Figure 12: LFB stained brain tissue of the focal EAE rat model. (A)** The pink colour illustrates the demyelination in the cortex (Magnification: x100). **(B)** Detailed View of the cortex. The pink area shows the demyelination in the cortex (Magnification: x200).

This aspect of demyelination is confirmed by the immunohistochemistry of the myelin component PLP in figure 13. The brown signal loss in figure 13 indicates the demyelination in the cortex. Only the blue counterstaining of the cell nuclei are visible in the cortical area at high magnification (Fig 13 B, C). This demyelination looks remarkably similar to those found in human cortical lesions in MS in extreme cases.



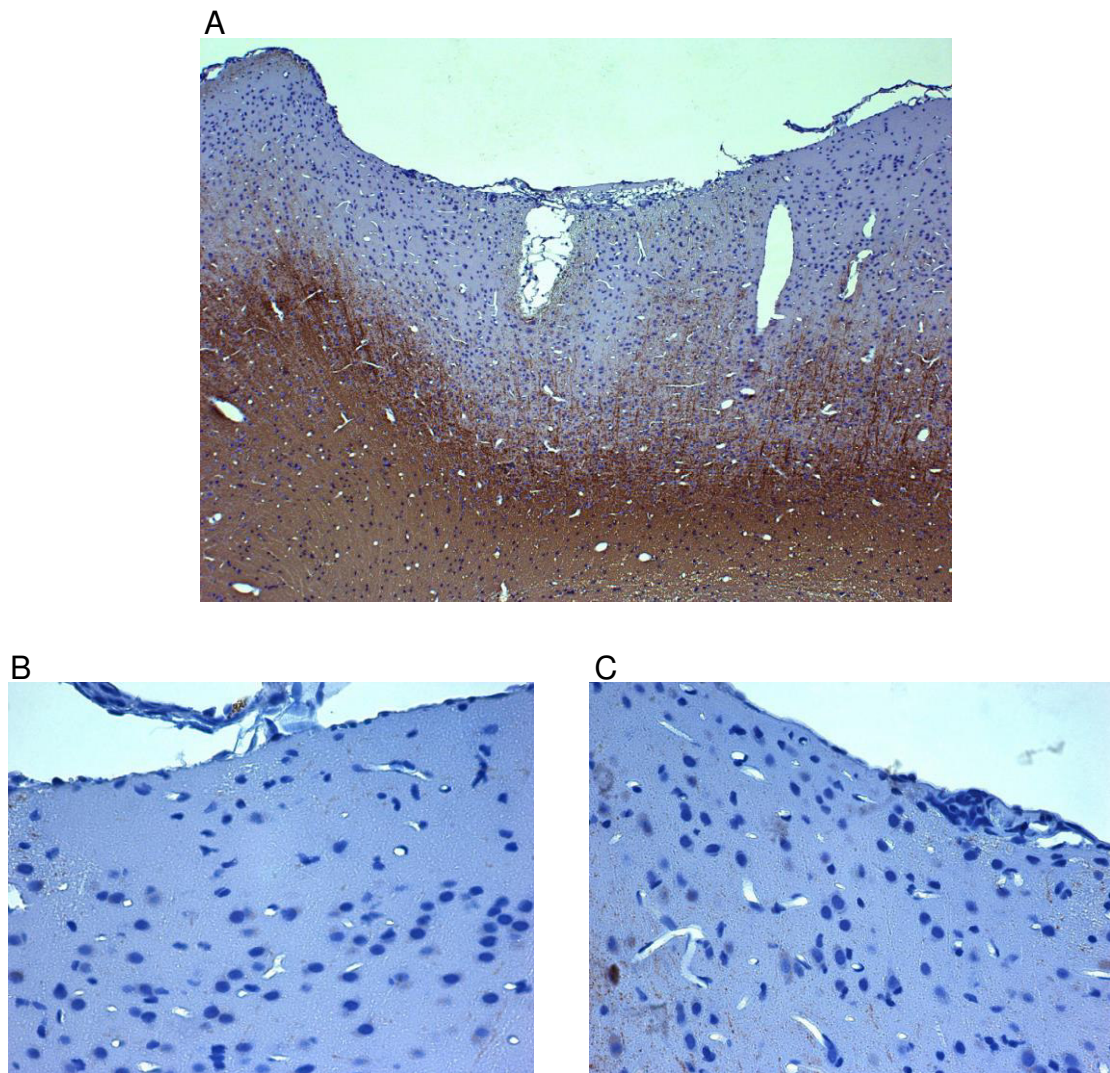


**Figure 13: PLP-IHC stained brain tissue of the focal EAE rat model. (A)** The absence of the brown signal of the PLP-IHC indicates demyelination in the area of the cortex (Magnification: x100). **(B)** Detailed view of the PLP-IHC stained brain tissue. The brown signal is lost in the cortex (Magnification: x630). **(C)** Detailed view of the PLP-IHC stained cortex. There is no brown signal visible (Magnification: x630).

There were no signs of demyelination in the spinal cord (figure 14) in our animals, which would be the hallmark of any conventional standard EAE model. Figure 14 A shows the HE stained spinal cord of the same animal. There are neither lesions nor cellular infiltrates visible. The LFB stained spinal cord in figure 14 B appears normal with intact myelin staining signal. The immunohistochemistry of PLP (figure 14 C) also does not show any brown signal loss. So the spinal cord does not have any sign of demyelination. In contrast to this the standard EAE model shows a widespread demyelination in the spinal cord (see for comparison figure 3, at page 9).

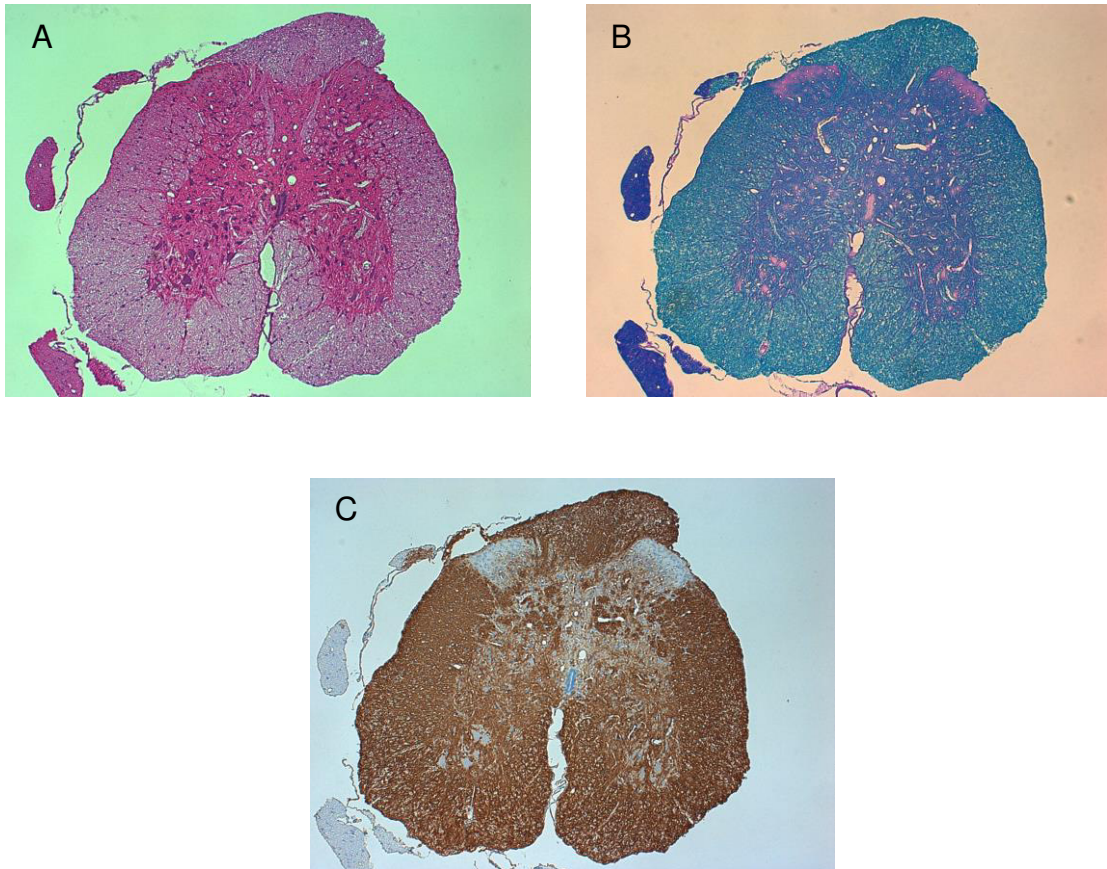


**Figure 14: Focal cortical EAE stained with HE, LFB and PLP-IHC.** (All pictures were taken with a 100-fold magnification) **(A)** Spinal cord of the focal EAE that is stained with HE. There are no lesions or cellular infiltrates visible. **(B)** LFB stained spinal cord of the focal EAE. There is no demyelination visible. The spinal cord appears to be normal. **(C)** PLP-IHC of the spinal cord of the focal EAE. There is no signal loss in this picture. The spinal cord does not have any damage.

Therefore we conclude that we were able to achieve cortical lesions (figure 12 and 13) in our rats without any signs of demyelination in the spinal cord (figure 14).

In those two animals which had to be sacrificed due to breathing problems on day 9 we found, additional to demyelination in the cortex, also a widespread demyelination in the brain stem, which explains the symptoms very well. Most likely this occurred due to an overshoot reaction.

## 6.5 Post mortem MRI scans

Histology results prompted us to try post-mortem MRI of the brains to assess if there are any scan settings that enable us to see equivalent lesions as in histology. Post mortem scans of the brains allow virtually unlimited scanning times and testing of multiple different setting without any animal welfare concerns.

The results of these MRI scans, performed overnight in Galden, are shown in figure 15 and 16).



**Figure 15:** Post mortem  $T_2$ -weighted MRI scan of the rat brain. The image shows frame 11 and 12.



**Figure 16:** Post mortem  $T_2$ -weighted MRI scan of the rat brain. Frame 13 and 14 are shown in this image.

We assume that the slightly lighter “rim” along the cortex might depict the cortical lesion. However MRI resolution might be too low to depict an area that small.

## 7. Discussion

In this study we were able to create a new animal model of focal cortical EAE. Of course the data presented here is only preliminary and more experiments to increase the animal number and to demonstrate the development of the cortical lesion from very early to very late time points are currently ongoing. Also, a detailed histological examination of all lesion stages with respect to all cell types and axonal changes is necessary.

Based on the currently available data our animal model is able to produce cortical lesions that are histologically remarkably similar to human cortical demyelination in MS, which are increasingly found in later stages of the disease.

The cortical lesions are much more difficult to detect with an MRI, also in human disease. They are less likely to be visible on T<sub>2</sub>-weighted images than those in white matter because grey matter lesions have longer relaxation times. This results in a poor contrast resolution between grey matter and cortical lesions compared with lesions and white matter. There are partial volume effects with the surrounding CSF outside the cortex which should be considered too. The cellular density of cortical lesions might be the most important difference compared to white matter lesions. It is possible that the high cellular density does not allow an adequate expansion of the extracellular space to allow an increase of relaxation times in cortical lesions than those arising in white matter (Kidd, et al., 1999).

Moreover we were just showing serial T<sub>2</sub>-weighted MRI scans of the rat brain. We had a very limited measurement time of 30 minutes in the living animals, which is of course affecting the resolution. However we saw an edema at day 6 in one animal that was definitely not caused by the cytokine injection itself. Unfortunately we were not able to detect a cortical lesion with MRI scans. As we were searching in a very small area of the brain, the viewing angle could play a very important role in finding a cortical lesion too. Taken together, the fact that we did not see much of the lesions in T<sub>2</sub> weighted images in the living animals should not come as too much of a surprise. The signal we see in the post mortem scans still has to be confirmed and tested as at this moment we had only two brains available for post mortem scanning.

Previous studies such as Merkler et al. were able to generate a model of focal cortical EAE too. However they injected the cytokines via stereotactic cortical injection. This method causes a trauma and is very unclear. Also, they only achieved a tiny cortical lesion in the injected hemisphere only. Reproducibility is also a big problem. You cannot be sure whether a lesion is just forming because of the injection or how many animals even get a lesion with this method alone as any injection trauma would also open the blood brain barrier and cause blood cells to come into the injected area in a preimmunized animal. In contrast to this our technique did not cause a second trauma as we injected the cytokines via the implanted catheter at a rate that is actually even slower than



the rate of interstitial fluid turnover of 1µl in 10 minutes as found in the literature. Therefore, we assume that our injection method is actually based on diffusion and not really an actual injection.

We were able to demonstrate the proof of principle with this study. Nevertheless we had to do a lot of troubleshooting to come that far. For instance the sensitization procedure is very difficult. We had to find the right concentration of MOG. A higher concentration can make the animals very sick and they have to be sacrificed immediately. Once this step succeeded we had to find an ideal range of the anti-MOG serum titers. The serum titers should always be controlled. After some time the serum titers will drop and it is possible that there is a second injection of MOG necessary to maintain a sufficient antibody titer.

Our focal cortical EAE model is not identical with the standard animal model of EAE. In case of the standard EAE there are severe lesions in the spinal cord. This leads to an ascending paralysis of the legs. The animals are suffering and therefore it is nearly impossible to have long term surveillance or test duration due to ethical reasons. The no-go criteria are the complete paralysis of the hind legs, which can happen really fast. In contrast to this the spinal cord of our focal cortical EAE model appears to be normal and not demyelinated on histological examination. Clinical symptoms tended to mild and temporary and most often were restricted to a diffuse slowing of the animals for a few days.

In summary, we were able to create a new animal model of focal cortical EAE. This model is much more similar to the human MS than the standard EAE model when it comes to the later stages of the disease. It is possible to perform long term surveillance and tests, since the implanted catheter itself does not cause any tissue reaction in the rat and clinical symptoms are much milder than in conventional EAE models. Due to the implanted catheter we do not cause a trauma when injecting the cytokines. This is a great advantage, because we can be sure that the lesion is forming as a result of the cytokines and nothing else. In addition we have access to the lesions in the living rat due to the implanted catheter. Although further research is required to find the right MRI parameters and to smooth out the experimental protocol to minimize the incidence of over-

shoot reactions this model could serve as a very valuable tool to test potential therapeutic drugs directly in the brain tissue.

## 8. List of figures

**Figure 1: CNS myelin and its components. (A)** An oligodendrocyte and myelin sheath in the CNS is shown. This version is simplified and has fewer myelin sheaths per oligodendrocyte. **(B)** 3D molecular composition of CNS myelin. Myelin proteins (MAG, MOG, PLP, MBP and CNP) are shown in yellow. The occurring lipids are: cholesterol in orange, phospholipids in pink and glycosphingolipids in blue. CNP: 2'3'-cyclic-nucleotide 3'-phosphodiesterase; FMC: Fast-migrating cerebroside; GalCer: Galactosylceramide; GM<sub>1</sub>: Monosialoganglioside; GM<sub>4</sub>: Sialosylgalactosylceramide; MAG: Myelin-associated glycoprotein; MBP: Myelin basic protein; MOG: Myelin oligodendrocyte glycoprotein; PLP: Proteolipid protein; sGalCer: Sulfatide..... 3

**Figure 2: Formation of the myelin sheath. (A)** The myelin sheath is formed by oligodendrocytes in the CNS. One oligodendrocyte is able to myelinate many axons. **(B)** Schwann cells form the myelin sheath in the PNS. One Schwann cell can only myelinate one axon. Obtained from:[http://medcell.med.yale.edu/systems\\_cell\\_biology\\_old/nervous\\_system.php](http://medcell.med.yale.edu/systems_cell_biology_old/nervous_system.php) (11.12.2015) ..... 4

**Figure 3: Standard EAE stained with haematoxylin and eosin (HE), luxol fast blue (LFB) and PLP-immunohistochemistry (PLP-IHC).** (All pictures were taken with a 100-fold magnification) **(A)** This HE staining shows the spinal cord of a standard EAE. There are many cellular infiltrates visible. **(B)** Spinal cord of the standard EAE stained with LFB. In this picture a widespread demyelination manifests itself in the pink colour of the LFB staining. **(C)** PLP-IHC of the spinal cord of the normal EAE. The missing brown signal of the PLP-IHC can be interpreted as a widespread demyelination..... 10

**Figure 4: Schema of the rat brain.** The grey bar illustrates the placement of the catheter. Adapted from: <http://learn.genetics.utah.edu/content/addiction/mice/> (11.12.2015)..... 19

**Figure 5: Labelled (strept-)avidin-biotin (L(S)AB) method.** The tissue antigen (shown in dark blue) is specifically bound by the unlabelled primary



antibody (green). The secondary antibody has to be biotinylated and binds to the primary antibody. Biotin (blue triangle) binds avidin (red) with a high affinity. Avidin is labelled with an enzyme (light blue spheres). In this study horseradish peroxidase (HRP) was used as an enzyme. It is responsible for the visualisation step. Obtained from:<http://www.dako.com/at/ihc-guidebook-detection-methods-chapter6.pdf> (11.12.2015) ..... 26

**Figure 6: HE and LFB staining of rat brain. (A)** HE staining of the rat brain tissue. There are no signs of any tissue reaction near the implanted catheter. (Magnification: x50) **(B)** LFB staining of the rat tissue. LFB is usually used to stain myelin. In this case demyelination, around the implanted catheter, does not occur. The animal was sacrificed 4 weeks after the implantation. (Magnification: x50) ..... 29

**Figure 7: PLP-IHC of the rat brain. (A)** PLP-IHC was performed on this rat brain tissue. The rat was sacrificed after 4 weeks after catheter implantation. PLP is detectable around the catheter channel in a normal density. (Magnification: x50) **(B)** Detailed view of the “lower” part of the rat cortex. (Magnification: x200) **(C)** Detailed view of the “upper” part of the rat cortex. (Magnification: x200). Please note the physiological differences in myelin density in the cortex area..... 30

**Figure 8: T<sub>2</sub>-weighted baseline of the rat brain.** This image shows the frames 17 and 18. In frame 18 the channel of the implanted catheter is visible. .... 31

**Figure 9: T<sub>2</sub>-weighted MRI scan of the rat brain at day 6.** This image shows the frames 15 and 16, where the channel of the implanted catheter is visible. At day 6 we were able to detect an edema at the region of the cortex in this rat brain..... 31

**Figure 10: T<sub>2</sub>-weighted MRI scan of the rat brain at day 10.** The frames 15 and 16 are shown. The channel of the implanted catheter is visible in frame 16. Cortical lesions were not detectable. .... 32

**Figure 11: T<sub>2</sub>-weighted MRI scan of the rat brain at day 13.** This image shows the frames 13 and 14. At day 13 there are no signs of cortical lesions visible..... 32

- Figure 12: LFB stained brain tissue of the focal EAE rat model. (A)** The pink colour illustrates the demyelination in the cortex (Magnification: x100). **(B)** Detailed View of the cortex. The pink area shows the demyelination in the cortex (Magnification: x200)..... 33
- Figure 13: PLP-IHC stained brain tissue of the focal EAE rat model. (A)**The absence of the brown signal of the PLP-IHC indicates demyelination in the area of the cortex (Magnification: x100). **(B)** Detailed view of the PLP-IHC stained brain tissue. The brown signal is lost in the cortex (Magnification: x630). **(C)** Detailed view of the PLP-IHC stained cortex. There is no brown signal visible (Magnification: x630). ..... 34
- Figure 14: Focal cortical EAE stained with HE, LFB and PLP-IHC.** (All pictures were taken with a 100-fold magnification) **(A)** Spinal cord of the focal EAE that is stained with HE. There are no lesions or cellular infiltrates visible. **(B)** LFB stained spinal cord of the focal EAE. There is no demyelination visible. The spinal cord appears to be normal. **(C)** PLP-IHC of the spinal cord of the focal EAE. There is no signal loss in this picture. The spinal cord does not have any damage. .... 35
- Figure 15: Post mortem T<sub>2</sub>-weighted MRI scan of the rat brain.** The image shows frame 11 and 12..... 36
- Figure 16: Post mortem T<sub>2</sub>-weighted MRI scan of the rat brain.** Frame 13 and 14 are shown in this image. .... 37

## 9. List of references

- Baron, Wia; Ozgen, Hande; Klunder, Bert; de Jonge, Jenny C.; et al. 2015.** The Major Myelin-Resident Protein PLP Is Transported to Myelin Membranes via a Transcytotic Mechanism: Involvement of Sulfatide. *Molecular and Cellular Biology*. 2015, 35(1), 288-302, (doi:10.1128/MCB.00848-14).
- Baum, Anke; Pohlmeier, Gabriele; Rapp, Karl, G.; Deerberg, Friedrich. 1995.** Lewis rats of the inbred strain LEW/Han: Life expectancy, spectrum and incidence of spontaneous neoplasms. *Experimental and Toxicologic Pathology*. 1995, 47 (1), 11-18, (doi:10.1016/S0940-2993(11)80275-7).
- Calabrese, Massimiliano; Poretto, Valentina; Favaretto, Alice; Alessio, Sara; et al. 2012.** Cortical lesion load associates with progression of disability in multiple sclerosis. *Brain*. 2012, 135 (10), 2952-61, (doi: 10.1093/brain/aws246).
- Charles, River. 2016.** *Research Animal Model - Lewis Rat*. [Online] Charles River, 2016. [Zitat vom: 02. Februar 2016.] <http://www.criver.com/products-services/basic-research/find-a-model/lewis-rat>.
- Compston, Alastair; Ebers, George; Lassmann, Hans; McDonald, Ian; et al. 1998.** *McAlpine's Multiple Sclerosis*. London : Churchill Livingstone, 1998. Thrid Edition, ISBN: 0 443 050082.
- Constantinescu, C. S.; Farooqi, N.; O'Brien, K.; Gran, B. 2011.** Experimental autoimmune encephalomyelitis (EAE) as a model for multiple sclerosis (MS). *British Journal of Pharmacology*. 2011, 164(4), 1079–1106, (doi: 10.1111/j.1476-5381.2011.01302.x).
- Furlan, Roberto; Cuomo, Carmela and Martino, Gianvito. 2009.** *Animal Models of Multiple Sclerosis*. [Buchverf.] Neil J. Scolding und David Gordon. *Neural Cell Transplantation Methods and Protocols*. New York : Humana Press, a part of Springer Science+Business Media, 2009.
- Geisseler, Olivia; Pflugshaupt, Tobias; Bezzola, Ladina; Reuter, Katja; et al. 2016.** Cortical thinning in the anterior cingulate cortex predicts multiple sclerosis patients' fluency performance in a lateralised manner. *NeuroImage : Clinical*. 2016, 10, 89-95, (doi: 10.1016/j.nicl.2015.11.008).

- Harlow, D. E.; Honce, J. M. and Miravalle, A. A. 2015.** Remyelination Therapy in Multiple Sclerosis. *Frontiers in Neurology*. 2015, 6, 257, (doi: 10.3389/fneur.2015.00257).
- Hermey, Guido; Mahlke, Claudia; Schwake, Michael; Sommer, Tobias. 2010.** *Der Experimentator: Neurowissenschaften*. Heidelberg : Spektrum Akademischer Verlag, 2010. ISBN: 978-3-8274-2368-9.
- Höftberger, Romana; Leisser, Marianne; Bauer, Jan; Lassmann, Hans. 2015.** Autoimmune encephalitis in humans: how closely does it reflect multiple sclerosis ? *Acta Neuropathologica Communications*. 2015, 3, 80, (doi: 10.1186/s40478-015-0260-9).
- Humphrey, Peter A.; Dehner, Louis P. and Pfeifer, John D. 2008.** *The Washington Manual of Surgical Pathology*. Missouri : Lippincott Williams & Wilkins, 2008. ISBN: 978-0-7817-6527-5.
- Hutchings, P., R.; Varey, A., M. and Cooke, A. 1986.** Immunological defects in SJL mice. *Immunology*. 1986, 59 (3), 445-450.
- JAX®, Mice strain SJL/J. 2016.** *Mouse Strain Datasheet - 000686*. [Online] Jackson Laboratory JAX® Mice Database, 2016. [Zitat vom: 1. Februar 2016.] <https://www.jax.org/strain/000686>.
- Joy, JE; Johnston, RB Jr.; editors. 2001.** *Institute of Medicine (US) Committee on Multiple Sclerosis: Current Status and Strategies for the Future*. Washington (DC) : National Academies Press (US), 2001. Available from: <http://www.ncbi.nlm.nih.gov/books/NBK222386/>.
- Kidd, D.; Barkhof, F.; McConnell, R.; Algra, P. R.; et al. 1999.** Cortical lesions in multiple sclerosis. *Brain*. 1999, 122 (1), 17-26, (doi:10.1093/brain/122.1.17).
- Kondo, Takayuki; Yamamura, Takashi; Inobe, Jun-ichi; Ohashi, Takashi; et al. 1996.** TCR repertoire to proteolipid protein (PLP) in multiple sclerosis (MS): homologies between PLP-specific T cells and MS associated T cells in TCR junctional sequences. *International Immunology*. 1996, 8 (1), 123-130, (doi: 10.1093/intimm/8.1.123).
- Kumar, Rakesh K. 1983.** Hodgkin's disease. SJL/J murine lymphoma. *The American Journal of Pathology*. 1983, 110 (3), 393-396.

- Luttmann, Werner; Bratke, Kai; Küpper, Michael; Myrtek, Daniel. 2014.** *Der Experimentator Immunologie*. Berlin Heidelberg : Springer Spektrum, 2014. ISBN: 978-3-642-41899-0.
- Marro, B. S.; Blanc, C. A.; Loring, J. F.; Cahalan, M. D. et al. 2014.** Promoting remyelination: utilizing a viral model of demyelination to assess cell-based therapies. *Expert Review of Neurotherapeutics*. 2014, 14(10), 1169-1179, (doi:10.1586/14737175.2014.955854).
- Merkler, Doron; Ernsting, Tristan; Kerschensteiner, Martin; Brück, Wolfgang; et al. 2006.** A new focal EAE model of cortical demyelination: multiple sclerosis-like lesions with rapid resolution of inflammation and extensive remyelination. *Brain*. 2006, 129, 1972 - 1983, (doi: 10.1093/brain/aw1135).
- Mix, Eilhard, Meyer-Rienecker, Hans; Hartung, Hans-Peter; Zettl, Uwe, K. 2010.** Animal models of multiple sclerosis—Potentials and limitations. *Progress in Neurobiology*. 2010, 92 (3), 386-404, (doi: 10.1016/j.pneurobio.2010.06.005).
- Murray, T. Jock. 2005.** *Multiple Sclerosis: The History of a Disease*. New York : Demos Medical Publishing, 2005. ISBN: 1-888799-80-3.
- Nave, Klaus-Armin. 2003.** Neuron-Glia-Interaktion: Mausmutanten der Myelinbildung. *Jahrbuch - Max-Planck-Institut für experimentelle Medizin*. 2003, Available from: [https://web.archive.org/web/20051102091445/http://www.mpg.de/bilderBerichteDokumente/dokumentation/jahrbuch/2003/experimentelle\\_medizin/forschungsSchwerpunkt/index.html](https://web.archive.org/web/20051102091445/http://www.mpg.de/bilderBerichteDokumente/dokumentation/jahrbuch/2003/experimentelle_medizin/forschungsSchwerpunkt/index.html) (28.01.2016).
- Procaccini, Claudio; De Rosa, Veronica; Pucino, Valentina; Formisano, Luigi; et al. 2015.** Animal models of Multiple Sclerosis. *European Journal of Pharmacology*. 2015, 759, 182 - 191, (doi:10.1016/j.ejphar.2015.03.042).
- Rasband, Matthew N. 2015.** Glial Contributions To Neural Function And Disease. *Molecular & Cellular Proteomics*. 2015, 15 (2), 355-361, (doi: 10.1074/mcp.R115.053744).
- Robinson, Andrew, P.; Harp, Christopher, T.; Noronha, Avertano; Miller, Stephen, D. 2014.** The experimental autoimmune encephalomyelitis (EAE) model of MS: utility for understanding disease pathophysiology and treatment. *Handbook of Clinical Neurology*. 2014, 122, 173-189, (doi: 10.1016/B978-0-444-52001-2.00008-X).

- Shin, Taekyun; Ahn, Meejung and Matsumoto, Yoh. 2012.** Mechanism of experimental autoimmune encephalomyelitis in Lewis rats: recent insights from macrophages. *Anatomy and Cell Biology*. 2012, 45(3), 141-148, (doi: <http://dx.doi.org/10.5115/acb.2012.45.3.141>).
- Siegel, George J.; Agranoff, Bernard W.; Albers, R. Wayne; Fisher, Stephen K.; et al. 1999.** *Basic Neurochemistry Molecular, Cellular and Medical Aspects*. Philadelphia : Lippincott - Raven, 1999. ISBN-10: 0-397-51820-X.
- Sriram, Subramaniam and Steiner, Israel. 2005.** Experimental Allergic Encephalomyelitis: A Misleading Model of Multiple Sclerosis. *Annals of Neurology*. 2005, 58 (6), 939-945, (doi: 10.1002/ana.20743).
- Taconic. 2016.** *Rat Model - Dark Agouti*. [Online] Taconic Biosciences, 2016. [Zitat vom: 02. Februar 2016.] <http://www.taconic.com/rat-model/dark-agouti>.
- Takano-Maruyama, M.; Ohara, Y.; Asakura, K.; Okuwa, T. 2006.** Leader (L) and L\* proteins of Theiler's murine encephalomyelitis virus (TMEV) and their regulation of the virus' biological activities. *Journal of Neuroinflammation*. 2006, 3, 19, (doi:10.1186/1742-2094-3-19).
- Vafiadaki, E.; Reis, A.; Keers, S.; Harrison, R.; et al. 2001.** Cloning of the mouse dysferlin gene and genomic characterization of the SJL-Dysf mutation. *Neuroreport*. 2001, 12 (3), 625-629.
- Wekerle, H. 2008.** Lessons from multiple sclerosis: models, concepts, observations. *Annals of the Rheumatic Diseases*. 2008, 67 (3), 56-60, (doi: 10.1136/ard.2008.098020).
- Weller, A., H.; Magliato, S., A.; Bell, K., P.; Rosenberg, N., L. 1997.** Spontaneous myopathy in the SJL/J mouse: pathology and strength loss. *Muscle & Nerve*. 1997, 20 (1), 72-82, (doi: 10.1002/(SICI)1097-4598(199701)20:1<72::AID-MUS10>3.0.CO;2-3).